THE JOURNAL OF PHYSICAL CHEMISTRY A

Article

pubs.acs.org/JPCA

Economical Doubly Electron-Attached Equation-of-Motion Coupled-Cluster Methods with an Active-Space Treatment of Three-Particle–One-Hole and Four-Particle–Two-Hole Excitations

Published as part of The Journal of Physical Chemistry virtual special issue "Mark S. Gordon Festschrift".

Adeayo O. Ajala,[†] Jun Shen,[†] and Piotr Piecuch*[,†,‡]

[†]Department of Chemistry and [‡]Department of Physics and Astronomy, Michigan State University, East Lansing, Michigan 48824, United States

ABSTRACT: The previously developed active-space doubly electron-attached (DEA) equation-of-motion (EOM) coupled-cluster (CC) method with up to four-particle–two-hole (4p-2h) excitations [Shen, J.; Piecuch, P. *J. Chem. Phys.* **2013**, 138, 194102], which utilizes the idea of applying a linear electron-attaching operator to the CC ground state of an $(N-2)$-electron closed-shell system to generate ground and excited states of the N-electron open-shell species of interest, has been extended to a considerably less expensive model, in which both 3p-1h and 4p-2h terms rather than 4p-2h contributions only are selected using active orbitals. As illustrated by the calculations involving low-lying singlet and triplet states of methylene, trimethylenemethane, cyclobutadiene, and cyclopentadienyl cation and bond breaking in F_2, the proposed DEA-EOMCC method with the active-space treatment of 3p-1h and 4p-2h excitations and its lower-level counterpart neglecting 4p-2h contributions are capable of accurately reproducing the results obtained using their considerably more expensive parent counterparts with a full treatment of 3p-1h and full or active-space treatment of 4p-2h excitations.

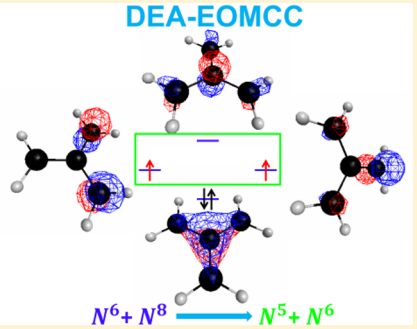

1. INTRODUCTION

Quantum chemistry methods based on the exponential wave function ansatz[1,2] of the single-reference coupled-cluster (CC) theory[3−8] and their extensions to excited states and properties other than energy exploiting the equation-of-motion (EOM)[9−13] and linear response[14−21] frameworks have witnessed considerable success in a wide range of molecular applications.[22,23] This includes extensions of the EOMCC formalism to open-shell systems obtained by adding electron(s) to or removing electron(s) from the corresponding closed-shell cores via the electron-attached (EA)[24−30] or ionized (IP)[26,28−38] methodologies, their linear response[39] and symmetry-adapted-cluster configuration interaction (CI)[40−43] counterparts, and their multiply attached/ionized generalizations, such as the doubly electron-attached (DEA) and doubly ionized (DIP) EOMCC schemes[44−52] or the EOMCC approach to triple electron attachment.[53] There is growing interest in the EA/IP-EOMCC, DEA/DIP-EOMCC, and similar approaches, as a way to handle ground and excited states of open-shell species around closed shells, such as radicals and biradicals, in an accurate and rigorously spin-adapted manner.

Recently, our group developed high-level variants of the DEA- and DIP-EOMCC approaches with up to four-particle–two-hole (4p-2h) and four-hole–two-particle (4h-2p) excitations, abbreviated as DEA-EOMCC(4p-2h) and DIP-EOMCC(4h-2p), respectively, and their less expensive active-space counterparts, designated as DEA-EOMCC(4p-2h)$\{N_u\}$ and DIP-EOMCC(4h-2p)$\{N_o\}$, where N_u and N_o indicate the numbers of active unoccupied and active occupied orbitals used to select the corresponding 4p-2h and 4h-2p contributions, as promising new ways to describe multireference systems having two electrons outside the corresponding closed-shell cores.[51,52] The DEA-EOMCC(4p-2h)$\{N_u\}$ and DIP-EOMCC(4h-2p)$\{N_o\}$ approaches of refs 51 and 52 have been shown to be highly successful in challenging test cases involving single bond breaking in closed-shell molecules leading to doublet dissociation fragments and electronic spectra of biradicals, almost perfectly reproducing the parent full DEA-EOMCC(4p-2h) and DIP-EOMCC(4h-2p) data at the small fraction of the computer cost, but even with the help of active orbitals to select the dominant 4p-2h excitations, calculations at the DEA-EOMCC(4p-2h) level remain quite expensive, especially when larger basis sets are employed. This has encouraged us to investigate economical approximations to the existing active-space DEA-EOMCC(4p-2h)$\{N_u\}$ and full DEA-EOMCC(4p-2h) methods,[51,52] capable of maintaining high accuracies the DEA-EOMCC(4p-2h)-level theories offer.

To better appreciate the benefits the new DEA-EOMCC methods proposed and tested in this work offer, let us examine computer costs of the DEA-EOMCC(4p-2h) calculations. The most expensive central processing unit (CPU) operations of

Received: November 11, 2016
Revised: April 13, 2017
Published: April 14, 2017

DOI: 10.1021/acs.jpca.6b11393
J. Phys. Chem. A 2017, 121, 3469−3485

the DEA-EOMCC(4p-2h) computations with a full treatment of 3p-1h and 4p-2h contributions scale as $n_o^2 n_u^6$, where n_o and n_u are the numbers of occupied and unoccupied orbitals, respectively, or as $\mathcal{N}^8$ with the system size $\mathcal{N}$ (see refs 51 and 52). As a result, the DEA-EOMCC(4p-2h) approach, although highly accurate in applications involving single bond breaking in closed-shell molecules and biradical electronic spectra,[51,52] is usually prohibitively expensive (for the examples of timings, see Section II.B of ref 51). The active-space DEA-EOMCC(4p-2h)$\{N_u\}$ approach, which uses a subset of N_u unoccupied orbitals to select the dominant 4p-2h excitations, reduces the most expensive $n_o^2 n_u^6$ steps of full DEA-EOMCC-(4p-2h) to a considerably more manageable $N_u^2 n_o^2 n_u^4$ or $\sim\mathcal{N}^6$ level, equivalent to costs of the standard EOMCC calculations with singles and doubles (EOMCCSD)[10−12] or costs of the ground-state CCSD computations[54,55] times a relatively small prefactor if $N_u \ll n_u$, but this does not solve the problem in its entirety. Indeed, the DEA-EOMCC(4p-2h)$\{N_u\}$ calculations remain quite expensive, since the lower-rank 3p-1h components are still treated in them fully using all orbitals in the basis set, which is a serious problem in applications using larger basis sets. The full treatment of 3p-1h excitations within the DEA-EOMCC framework requires CPU steps that scale as $n_o n_u^5$, which can be as demanding as or, in some cases, more time-consuming than the $N_u^2 n_o^2 n_u^4$ steps of the DEA-EOMCC(4p-2h)$\{N_u\}$ method associated with 4p-2h terms, especially when n_u becomes larger, since typical values of N_u and n_o are much smaller than n_u. The same analysis applies to the lower-level DEA-EOMCC(3p-1h) approach,[44,45,47,48,51,52] in which the electron-attaching operator of the DEA-EOMCC formalism is truncated at 3p-1h component. The DEA-EOMCC(3p-1h) calculations can be quite expensive too due to the $n_o n_u^5$ steps resulting from a full treatment of 3p-1h excitations.

In this article, we present a solution to the above problems by proposing and testing a new class of computationally affordable variants of the DEA-EOMCC approach, abbreviated as DEA-EOMCC(3p-1h)$\{N_u\}$ and DEA-EOMCC(3p-1h,4p-2h)$\{N_u\}$. In analogy to the DEA-EOMCC(4p-2h)$\{N_u\}$ and DIP-EOMCC(4h-2p)$\{N_o\}$ methods of refs 51 and 52 and their active-space CC,[56−67] EOMCC,[68−73] and EA/IP-EOMCC[28−30,43] predecessors (see ref 74 for a review), the DEA-EOMCC(3p-1h)$\{N_u\}$ and DEA-EOMCC(3p-1h,4p-2h)$\{N_u\}$ schemes developed in this work employ active orbitals to capture dominant excitation (in this case, electron attaching) amplitudes. Thus, the DEA-EOMCC(3p-1h)$\{N_u\}$ approach uses N_u active unoccupied orbitals to select a small subset of the dominant 3p-1h amplitudes within the standard DEA-EOMCC(3p-1h) framework. Similarly, the DEA-EOMCC(3p-1h,4p-2h)$\{N_u\}$ method uses N_u active unoccupied orbitals to select the dominant 3p-1h and 4p-2h amplitudes within the higher-level DEA-EOMCC(4p-2h) scheme. In other words, the DEA-EOMCC(3p-1h)$\{N_u\}$ approach is a natural approximation to its DEA-EOMCC(3p-1h) parent, which becomes full DEA-EOMCC(3p-1h) when all unoccupied orbitals in the basis set are active (i.e., $N_u = n_u$). Similarly, the DEA-EOMCC(3p-1h,4p-2h)$\{N_u\}$ approach is a natural approximation to its DEA-EOMCC(4p-2h) parent or to the DEA-EOMCC(4p-2h)$\{N_u\}$ method of refs 51 and 52, becoming full DEA-EOMCC(4p-2h) when $N_u = n_u$. The DEA-EOMCC(3p-1h)$\{N_u\}$ and DEA-EOMCC(3p-1h,4p-2h)$\{N_u\}$ approaches proposed in this work offer significant savings in the computer effort compared to their full DEA-EOMCC(3p-1h) and DEA-EOMCC(4p-2h) counterparts by reducing the expensive $\mathcal{N}^6$-like $n_o n_u^5$ steps associated with 3p-1h excitations to a $\mathcal{N}^5$-like $N_u n_o n_u^4$ level, which for larger systems is less expensive than costs of the underlying CCSD calculations. As in the case of the previously proposed DEA-EOMCC(4p-2h)$\{N_u\}$ approximation,[51,52] the DEA-EOMCC(3p-1h,4p-2h)$\{N_u\}$ method replaces the $\mathcal{N}^8$-like $n_o^2 n_u^6$ steps associated with 4p-2h contributions by the much more affordable, CCSD-type, $N_u^2 n_o^2 n_u^4$ steps, in addition to using the relatively inexpensive $\mathcal{N}^5$-like $N_u n_o n_u^4$ steps in handling 3p-1h terms.

To test the DEA-EOMCC(3p-1h)$\{N_u\}$ and DEA-EOMCC-(3p-1h,4p-2h)$\{N_u\}$ approaches, especially when compared to the previously examined[51,52] DEA-EOMCC(3p-1h), DEA-EOMCC(4p-2h)$\{N_u\}$, and DEA-EOMCC(4p-2h) methods, we investigate adiabatic excitation energies characterizing low-lying states of methylene, singlet−triplet gaps in trimethylenemethane (TMM), cyclobutadiene (CBD), and cyclopentadienyl cation (CPC), and bond breaking in the F_2 molecule. We show that the new DEA-EOMCC(3p-1h,4p-2h)$\{N_u\}$ approach with the active-space treatment of 3p-1h and 4p-2h excitations and its lower-level DEA-EOMCC(3p-1h)$\{N_u\}$ counterpart accurately reproduce the results obtained with the considerably more expensive parent DEA-EOMCC methods with a full treatment of 3p-1h and full or active-space treatment of 4p-2h excitations.

2. THEORY AND ALGORITHMIC DETAILS

2.1. The Existing DEA-EOMCC(3p-1h), DEA-EOMCC-(4p-2h), and DEA-EOMCC(4p-2h)$\{N_u\}$ Approximations. In the DEA-EOMCC formalism exploited in this work, one represents the ground and excited states $|\Psi_\mu^{(N)}\rangle$ of the N-electron system obtained by adding two electrons to the closed-shell core using the following wave function ansatz:[44,45,47,48,51,52]

$$|\Psi_\mu^{(N)}\rangle = R_\mu^{(+2)}|\Psi_0^{(N-2)}\rangle \tag{1}$$

where

$$|\Psi_0^{(N-2)}\rangle = e^T|\Phi^{(N-2)}\rangle \tag{2}$$

is the CC ground state of the $(N-2)$-electron closed-shell species, with $|\Phi^{(N-2)}\rangle$ designating the corresponding reference determinant that serves as a Fermi vacuum. The operator T entering eq 2 is the usual particle-conserving cluster operator, obtained in the ground-state CC calculations for the $(N-2)$-electron reference system, and

$$R_\mu^{(+2)} = \sum_{n=2}^{M_R} R_{\mu,\mathrm{np}\text{-}(n-2)\mathrm{h}} \tag{3}$$

where $M_R = N$ in the exact case and $M_R < N$ in approximate schemes is the EOM operator attaching two electrons to the corresponding $(N-2)$-electron closed-shell core, while allowing excitations of the remaining electrons via the $R_{\mu,\mathrm{np}\text{-}(n-2)\mathrm{h}}$ components with $n > 2$. Assuming that the highest many-body rank in T, designated as M_T, is at least $(M_R - 2)$, we obtain the $R_{\mu,\mathrm{np}\text{-}(n-2)\mathrm{h}}$ components of the $R_\mu^{(+2)}$ operator and the corresponding vertical electron-attachment energies

$$\omega_\mu^{(N)} = E_\mu^{(N)} - E_0^{(N-2)} \tag{4}$$

where $E_\mu^{(N)}$ is the energy of the N-electron state $|\Psi_\mu^{(N)}\rangle$ and $E_0^{(N-2)}$ is the ground-state CC energy of the $(N-2)$-electron

DOI: 10.1021/acs.jpca.6b11393
J. Phys. Chem. A 2017, 121, 3469−3485

reference system, by solving the following nonhermitian eigenvalue problem:[51,52]

$$(\bar{H}_{N,\mathrm{open}}R_\mu^{(+2)})_C|\Phi^{(N-2)}\rangle = \omega_\mu^{(N)}R_\mu^{(+2)}|\Phi^{(N-2)}\rangle \quad (5)$$

in the space of N-electron determinants corresponding to the $R_{\mu,n\mathrm{p}\text{-}(n-2)\mathrm{h}}$ components included in $R_\mu^{(+2)}$. Here, $\bar{H}_{N,\mathrm{open}}$ is the open part of the similarity-transformed form of the Hamiltonian H, written in the normal-ordered representation $H_N = H - \langle\Phi^{(N-2)}|H|\Phi^{(N-2)}\rangle$, that is, the open part of the

$$\bar{H}_N = e^{-T}H_Ne^T = (H_Ne^T)_C \quad (6)$$

operator obtained in the underlying CC calculations for the $(N-2)$-electron reference system, and subscript C designates the connected operator product. Thus, $\bar{H}_{N,\mathrm{open}}$ is this part of $\bar{H}_N$, eq 6, that corresponds to diagrams of $(H_Ne^T)_C$, which have external Fermion lines. It is easy to show that $\bar{H}_{N,\mathrm{open}} = \bar{H} - E_0^{(N-2)}\mathbf{1}$, where $\bar{H} = e^{-T}\,H\,e^T$ and $\mathbf{1}$ is the unit operator. As explained in refs 51 and 52 (cf. refs 13, 28−30, and 43 for an analogous discussion of the EA/IP cases), the aforementioned condition $M_R - 2 \le M_T$ is needed to obtain the connected form of the eigenvalue problem represented by eq 5, which is, in turn, important if we are to retain the desired size intensivity[19] of the resulting electron-attachment energies $\omega_\mu^{(N)}$.

Different truncations in the cluster and electron attaching operators, T and $R_\mu^{(+2)}$, respectively, satisfying the $M_R - 2 \le M_T$ condition, lead to various DEA-EOMCC schemes. In particular, in the DEA-EOMCC(4p-2h) method developed in refs 51 and 52, we truncate T at double excitations, so that $M_T = 2$, use the CCSD approach to determine the $(N-2)$-electron reference ground state $|\Psi_0^{(N-2)}\rangle$, and set M_R in eq 3 at 4, obtaining

$$R_\mu^{(+2)} = R_{\mu,2\mathrm{p}} + R_{\mu,3\mathrm{p}\text{-}1\mathrm{h}} + R_{\mu,4\mathrm{p}\text{-}2\mathrm{h}} \quad (7)$$

where

$$R_{\mu,2\mathrm{p}} = \sum_{a<b} r_{ab}(\mu)a^aa^b \quad (8)$$

$$R_{\mu,3\mathrm{p}\text{-}1\mathrm{h}} = \sum_{k,a<b<c} r_{abc}^{\ k}(\mu)a^aa^ba^ca_k \quad (9)$$

and

$$R_{\mu,4\mathrm{p}\text{-}2\mathrm{h}} = \sum_{k>l,a<b<c<d} r_{abcd}^{\ kl}(\mu)a^aa^ba^ca^da_la_k \quad (10)$$

are the relevant 2p, 3p-1h, and 4p-2h components. We determine these components, or the amplitudes $r_{ab}(\mu)$, $r_{abc}^{\ k}(\mu)$, and $r_{abcd}^{\ kl}(\mu)$ that represent them, along with the corresponding vertical electron-attachment energies $\omega_\mu^{(N)}$, eq 4, by diagonalizing the similarity-transformed Hamiltonian of CCSD obtained in the calculations for the $(N-2)$-electron reference system, given by eq 6 in which T is truncated at two-body clusters, in the space spanned by the N-electron $|\Phi^{ab}\rangle = a^aa^b|\Phi^{(N-2)}\rangle$, $|\Phi_k^{abc}\rangle = a^aa^ba^ca_k|\Phi^{(N-2)}\rangle$, and $|\Phi_{kl}^{abcd}\rangle = a^aa^ba^ca^da_la_k|\Phi^{(N-2)}\rangle$ determinants. The DEA-EOMCC(3p-1h) approach,[44,45,47,48] implemented in refs 51 and 52 as well, is obtained by neglecting the 4p-2h component of $R_\mu^{(+2)}$, $R_{\mu,4\mathrm{p}\text{-}2\mathrm{h}}$, in eq 7, that is, by setting M_R in eq 3 at 3. In this case, we diagonalize the similarity-transformed Hamiltonian of CCSD in the space spanned by the $|\Phi^{ab}\rangle$ and $|\Phi_k^{abc}\rangle$ determinants. Here and elsewhere in this article, we use the conventional notation in which i, j, k, l,... (a, b, c, d,...) indices are the spin−orbitals occupied (unoccupied) in the reference determinant $|\Phi^{(N-2)}\rangle$ and a^p (a_p) are the creation (annihilation) operators associated with the spin−orbital basis $\{|p\rangle\}$.

As is well-established and known for as long as the EOMCC theory has been in use, the diagonalization of the similarity-transformed Hamiltonian that accounts for the many-electron correlation effects originating from the underlying ground-state problem (in our case, correlations in the $(N-2)$-electron closed-shell core), which is the main characteristic of all EOMCC calculations, not only those performed in this work, offers great improvements in the accuracy of the resulting energies over the analogous CI-type diagonalizations of the bare Hamiltonian. In the specific context of the DEA-EOMCC considerations, the diagonalization of the bare Hamiltonian in the space defined by the truncated $R_\mu^{(+2)}$ operator, in addition to being much less accurate than the diagonalization of $\bar{H}$ or $\bar{H}_N$, destroys several fundamental properties, such as the aforementioned size intensivity of the resulting $\omega_\mu^{(N)}$ values. Indeed, the use of the bare Hamiltonian, H or H_N, instead of $\bar{H}$ or $\bar{H}_N$, formally means setting the cluster operator T (i.e., the value of M_T) at 0, which violates the condition $M_R - 2 \le M_T$ if $M_R \ge 3$, that is, when 3p-1h or higher-rank $R_{\mu,n\mathrm{p}\text{-}(n-2)\mathrm{h}}$ components are included in $R_\mu^{(+2)}$. We did compare the EOMCC-type and CI-type diagonalizations in the context of the EA and IP EOMCC considerations reported in ref 43, showing that the EA/IP CI diagonalizations of the bare Hamiltonian in the space up to 4p-3h or 4h-3p excitations are a lot less accurate than the corresponding EOMCC diagonalizations of $\bar{H}$ or $\bar{H}_N$. We illustrate the same point in a later part of this work at the various DEA levels up to 3p-1h and 4p-2h excitations.

As shown in refs 51 and 52, the full DEA-EOMCC(4p-2h) approach provides a virtually exact description of biradical electronic spectra, improving the results of the lower-level DEA-EOMCC(3p-1h) calculations, but this comes at a very high price of iterative $n_o^2n_u^6$ CPU steps and the need to store a large number of $\sim n_o^2n_u^4$ 4p-2h amplitudes $r_{abcd}^{\ kl}(\mu)$. It is, therefore, important to seek approximate treatments of 4p-2h contributions. One such treatment is offered by the active-space DEA-EOMCC(4p-2h)$\{N_u\}$ approach, which replaces the $R_{\mu,4\mathrm{p}\text{-}2\mathrm{h}}$ component in the many-body expansion of the DEA-EOMCC(4p-2h) electron-attaching operator $R_\mu^{(+2)}$, eq 7, by its active-space counterpart

$$r_{\mu,4\mathrm{p}\text{-}2\mathrm{h}} = \sum_{k>l,\mathbf{A}<\mathbf{B}<c<d} r_{\mathbf{AB}cd}^{\ kl}(\mu)a^{\mathbf{A}}a^{\mathbf{B}}a^ca^da_la_k \quad (11)$$

where the capital-case bold symbols $\mathbf{A}$ and $\mathbf{B}$ in eq 11 designate the active spin−orbitals unoccupied in the $(N-2)$-electron reference determinant $|\Phi^{(N-2)}\rangle$ (formally, any subset of unoccupied spin−orbitals, which we hope to be relatively small). The resulting $R_\mu^{(+2)}\{N_u\}$ operator defining the DEA-EOMCC(4p-2h)$\{N_u\}$ method is given by

$$R_\mu^{(+2)}\{N_u\} = R_{\mu,2\mathrm{p}} + R_{\mu,3\mathrm{p}\text{-}1\mathrm{h}} + r_{\mu,4\mathrm{p}\text{-}2\mathrm{h}} \quad (12)$$

where $R_{\mu,2\mathrm{p}}$, $R_{\mu,3\mathrm{p}\text{-}1\mathrm{h}}$, and $r_{\mu,4\mathrm{p}\text{-}2\mathrm{h}}$ are defined by eqs 8, 9, and 11, respectively. We obtain the relevant $r_{ab}(\mu)$, $r_{abc}^{\ k}(\mu)$, and $r_{\mathbf{AB}cd}^{\ kl}(\mu)$ amplitudes by diagonalizing the similarity-transformed Hamiltonian obtained in the CCSD calculations for the $(N-2)$-electron reference system in the subspace of the N-electron Hilbert space spanned by the $|\Phi^{ab}\rangle$, $|\Phi_k^{abc}\rangle$, and $|\Phi_{kl}^{\mathbf{AB}cd}\rangle$ determinants. If the number of active unoccupied orbitals N_u is small compared to the number of all unoccupied orbitals (n_u), the number of 4p-2h amplitudes to be determined in DEA-EOMCC(4p-2h)$\{N_u\}$ calculations, which equals the

DOI: 10.1021/acs.jpca.6b11393
J. Phys. Chem. A 2017, 121, 3469−3485

number of double excitations times a prefactor on the order of N_u^2, is much smaller than the number of all $r_{abcd}^{kl}(\mu)$ amplitudes ($\sim n_o^2 n_u^4$). This is precisely the source of savings in the computer effort offered by the active-space DEA-EOMCC(4p-2h)$\{N_u\}$ approach, when compared to full DEA-EOMCC(4p-2h).

2.2. The Active-Space DEA-EOMCC(3p-1h)$\{N_u\}$ and DEA-EOMCC(3p-1h,4p-2h)$\{N_u\}$ Approaches. The active-space DEA-EOMCC(4p-2h)$\{N_u\}$ method offers major savings in the computer effort compared to its full DEA-EOMCC(4p-2h) parent, replacing the prohibitively expensive $n_o^2 n_u^6$ steps of the latter approach by steps that scale as $N_u^2 n_o^2 n_u^4$, but, as explained in the Introduction, the CPU time associated with 3p-1h component $R_{\mu,3p\text{-}1h}$, which scales as $n_o n_u^5$, can be significant too, especially when larger basis sets are employed. To address this problem, in this paper we test a new, more economical variant of the active-space DEA-EOMCC(4p-2h) approach, designated DEA-EOMCC(3p-1h,4p-2h)$\{N_u\}$, in which both 3p-1h and 4p-2h components of the electron attaching operator $R_\mu^{(+2)}$, eq 7, are replaced by their active-space counterparts $r_{\mu,3p\text{-}1h}$ and $r_{\mu,4p\text{-}2h}$, respectively, to obtain a new form of the $R_\mu^{(+2)}$ operator, designated $\tilde{R}_\mu^{(+2)}\{N_u\}$ and defined as

$$\tilde{R}_\mu^{(+2)}\{N_u\} = R_{\mu,2p} + r_{\mu,3p\text{-}1h} + r_{\mu,4p\text{-}2h} \tag{13}$$

where $r_{\mu,4p\text{-}2h}$ is given by eq 11 and

$$r_{\mu,3p\text{-}1h} = \sum_{k,\mathbf{A}<b<c} r_{\mathbf{A}bc}^{\ k}(\mu) a^{\mathbf{A}} a^b a^c a_k \tag{14}$$

In analogy to eq 11, the capital-case bold index **A** in eq 14 runs over active spin−orbitals unoccupied in $|\Phi^{(N-2)}\rangle$. If we want to limit ourselves to the simpler DEA-EOMCC(3p-1h) level and reduce costs of the DEA-EOMCC(3p-1h) calculations further as well, we can consider the active-space variant of the DEA-EOMCC(3p-1h) approach, designated in this work as DEA-EOMCC(3p-1h)$\{N_u\}$, which is obtained by neglecting $r_{\mu,4p\text{-}2h}$ in eq 13. In defining the above $r_{\mu,3p\text{-}1h}$ component, we adopt the general philosophy of all active-space CC and EOMCC theories,[28−30,43,51,52,56−74] especially the previously formulated[51,52] DEA-EOMCC(4p-2h)$\{N_u\}$ method, emphasizing the dominant role of the lowest-energy unoccupied orbitals of the $(N-2)$-electron closed-shell core in the electron attachment process that leads to the formation of the N-electron biradical species of interest.

In analogy to the previously discussed full and active-space DEA-EOMCC(4p-2h) approaches,[51,52] in the DEA-EOMCC(3p-1h,4p-2h)$\{N_u\}$ calculations we determine the $R_{\mu,2p}$, $r_{\mu,3p\text{-}1h}$, and $r_{\mu,4p\text{-}2h}$ components of the electron attaching operator $\tilde{R}_\mu^{(+2)}\{N_u\}$, eq 13, by diagonalizing the similarity-transformed Hamiltonian $\bar{H}_{N,open}$ obtained in the CCSD calculations for the $(N-2)$-electron reference system, but now the diagonalization subspace is much smaller if $N_u \ll n_u$. Indeed, in the DEA-EOMCC(3p-1h,4p-2h)$\{N_u\}$ method, we diagonalize $\bar{H}_{N,open}$ in the subspace spanned by the $|\Phi^{ab}\rangle$, $|\Phi^{\mathbf{A}bc}_{\ k}\rangle$, and $|\Phi^{\mathbf{AB}cd}_{\ kl}\rangle$ determinants. Thus, instead of having to deal with $\sim n_o n_u^3$ 3p-1h and $\sim n_o^2 n_u^4$ 4p-2h amplitudes and determinants defining the eigenvalue problem of DEA-EOMCC(4p-2h), we consider $\sim N_u n_o n_u^2$ amplitudes and determinants of the 3p-1h type and $\sim N_u^2 n_o^2 n_u^2$ amplitudes and determinants of the 4p-2h type, which reflect on the content of $\tilde{R}_\mu^{(+2)}\{N_u\}$. This results in enormous savings in the computer effort compared to full DEA-EOMCC(4p-2h) calculations by reducing the expensive $n_o n_u^5$ steps associated with 3p-1h excitations and even more expensive $n_o^2 n_u^6$ steps associated with 4p-2h contributions to the much more affordable $N_u n_o n_u^4$ and $N_u^2 n_o^2 n_u^4$ levels. As shown in Section 2.3, the active-space DEA-EOMCC(3p-1h,4p-2h)$\{N_u\}$ approach proposed in this work is also substantially less expensive than its previously proposed[51,52] DEA-EOMCC(4p-2h)$\{N_u\}$ counterpart, which reduces the $n_o^2 n_u^6$ steps associated with 4p-2h excitations to the $N_u^2 n_o^2 n_u^4$ level, but treats 3p-1h contributions fully using expensive $n_o n_u^5$ CPU steps. Similar remarks apply to the active-space DEA-EOMCC(3p-1h)$\{N_u\}$ method, where we diagonalize $\bar{H}_{N,open}$ in the small subspace spanned by $|\Phi^{ab}\rangle$ and $|\Phi^{\mathbf{A}bc}_{\ k}\rangle$ determinants, so that instead of dealing with $\sim n_o n_u^3$ 3p-1h amplitudes and determinants defining the full DEA-EOMCC(3p-1h) eigenvalue problem, we consider a much smaller number of such amplitudes and determinants that scales as $\sim N_u n_o n_u^2$. As illustrated in Section 2.3, this leads to significant reductions in the CPU time needed to perform the DEA-EOMCC(3p-1h)-level calculations, since the CPU steps of DEA-EOMCC(3p-1h) that normally scale as $n_o n_u^5$ are replaced by the $N_u n_o n_u^4$ operations. Following our earlier remarks about EOMCC versus CI, it may be worth pointing out that the DEA-EOMCC(3p-1h,4p-2h)$\{N_u\}$ approach uses the same diagonalization space as its CI analogue, designated in this work as CI(3p-1h,4p-2h)$\{N_u\}$, which is essentially equivalent to the uncontracted multireference CI calculation in the same active space. The difference between the two methods is in the operator being diagonalized, which is the similarity-transformed Hamiltonian of CCSD in the former case and the bare Hamiltonian in the latter case. As shown in Section 3.1, the DEA-EOMCC(3p-1h,4p-2h)$\{N_u\}$ approach is much more accurate than its CI(3p-1h,4p-2h)$\{N_u\}$ counterpart.

2.3. Futher Details and Timings of DEA-EOMCC(3p-1h)$\{N_u\}$ and DEA-EOMCC(3p-1h,4p-2h)$\{N_u\}$ Calculations. In analogy to the previously developed DEA-EOMCC(3p-1h), DEA-EOMCC(4p-2h), and DEA-EOMCC(4p-2h)$\{N_u\}$ codes and their DIP counterparts described and tested in refs 51 and 52, our present computer implementation of the active-space DEA-EOMCC(3p-1h)$\{N_u\}$ and DEA-EOMCC(3p-1h,4p-2h)$\{N_u\}$ approaches proposed in this work has been interfaced with the atomic integral, restricted Hartree−Fock (RHF) as well as restricted open-shell Hartree−Fock (ROHF), and integral transformation routines available in the GAMESS package.[75,76] We benefited from the previously developed spin-free CCSD GAMESS routines,[77] which can use any set of orbitals and which help us solve the $(N-2)$-electron closed-shell CCSD equations prior to the DEA-EOMCC diagonalization steps, and from the routines that were used in some of our earlier EOMCC studies,[78−80] which provide us with the one- and two-body matrix elements of the similarity-transformed Hamiltonian of CCSD. Most importantly, in programming the DEA-EOMCC(3p-1h)$\{N_u\}$ and DEA-EOMCC(3p-1h,4p-2h)$\{N_u\}$ approaches, we took advantage of the explicit, computationally efficient equations defining the DEA-EOMCC(3p-1h) and DEA-EOMCC(4p-2h) eigenvalue problems in terms of one- and two-body matrix elements of the similarity-transformed Hamiltonian of CCSD and other recursively generated intermediates, reported in the appendix of ref 51, imposing suitable active-space logic on these equations with the help of our home-grown automated derivation and implementation software, which was previously exploited in coding the DEA-EOMCC(4p-2h)$\{N_u\}$ approach and its DIP counterpart[51] and a number of other CC/EOMCC methods that rely on similar logic, including those developed in refs 81−83. Further details, including the algorithms used to

DOI: 10.1021/acs.jpca.6b11393
J. Phys. Chem. A 2017, 121, 3469−3485

solve the DEA-EOMCC(3p-1h)$\{N_u\}$ and DEA-EOMCC(3p-1h,4p-2h)$\{N_u\}$ equations for the amplitudes defining the corresponding $R_\mu^{(+2)}$ operators and generate initial guesses, are similar to those reported in our earlier DEA-EOMCC work,[51,52] so they are not repeated here.

As already alluded to above, the active-space DEA-EOMCC-(4p-2h)$\{N_u\}$ method offers a massive reduction in computer effort compared to its DEA-EOMCC(4p-2h) parent with virtually no loss of accuracy. Indeed, as shown in ref 51, it is not unusual for the CPU timings of DEA-EOMCC(4p-2h)$\{N_u\}$ calculations to be hundreds of times smaller than the timings of the corresponding full DEA-EOMCC(4p-2h) computations. The DEA-EOMCC(3p-1h,4p-2h)$\{N_u\}$ approach developed in this study, which treats both 3p-1h and 4p-2h components of the $R_\mu^{(+2)}$ operator, not just the 4p-2h components, using active orbitals is even more economical. This is illustrated in Table 1,

Table 1. A Comparison of CPU Times Required by the Various DEA-EOMCC Calculations Characterizing the X $^3A_2'$ State of TMM, as Described by the cc-pVDZ and, in Parentheses, cc-pVTZ Basis Sets, along with the Formal Scalings of the Most Expensive Steps in the Diagonalization of $\bar{H}_{N,\mathrm{open}}$ with n_o, n_u, and N_u[a]

method	CPU time scaling	CPU time/iteration (min)[b]
DEA-EOMCC(3p-1h)$\{N_u\}$	$N_u n_o n_u^4$	0.05 (1.5)
DEA-EOMCC(3p-1h)	$n_o n_u^5$	0.43 (43.5)
DEA-EOMCC(3p-1h,4p-2h)$\{N_u\}$	$N_u^2 n_o^2 n_u^4 + N_u n_o n_u^4$	2.75 (65.0)
DEA-EOMCC(4p-2h)$\{N_u\}$	$N_u^2 n_o^2 n_u^4 + n_o n_u^5$	4.43 (136.0)

[a]The TMM^{2+} reference system used in the DEA-EOMCC calculations was obtained by vacating the doubly degenerate valence 1e″ orbitals of the TMM's π system (using the D_{3h} symmetry of the X $^3A_2'$ state). The lowest-energy core orbitals correlating with the 1s shells of the carbon atoms were frozen in the post-SCF calculations and the spherical components of the d and f orbitals were employed throughout. The active space used to select 3p-1h and 4p-2h components consisted of the doubly degenerate 1e″ and nondegenerate 2a$_2''$ orbitals, which are the three lowest-energy unoccupied MOs in the TMM^{2+} reference system, so N_u was set at 3. [b]The CPU time per iteration characterizing the DEA-EOMCC diagonalization step obtained on a single core of the PowerEdge R910 system from Dell using eight-core Intel Xeon X7560 2.26 GHz processor boards.

where we compare the CPU times per iteration characterizing the DEA-EOMCC diagonalization steps required by the full and active-space DEA-EOMCC(3p-1h) and active-space DEA-EOMCC(3p-1h,4p-2h)$\{N_u\}$ and DEA-EOMCC(4p-2h)$\{N_u\}$ calculations for the X $^3A_2'$ state of the TMM molecule, as described by the cc-pVDZ and cc-pVTZ basis sets,[84] which we also discuss in the next section.

We recall that we used the various DEA- and DIP-EOMCC methods to study the TMM system in refs 51 and 52. The TMM molecule is large enough to make the full DEA-EOMCC(4p-2h) calculations using the cc-pVDZ and cc-pVTZ basis sets prohibitively expensive, so the highest DEA-EOMCC level included in Table 1 is DEA-EOMCC(4p-2h)$\{N_u\}$. This is sufficient for the analysis presented here, since the CPU time savings offered by the active-space DEA-EOMCC(4p-2h)$\{N_u\}$ approach versus its full DEA-EOMCC(4p-2h) counterpart have already been discussed in refs 51 and 52. As one can see in Table 1, the DEA-EOMCC(3p-1h,4p-2h)$\{N_u\}$ calculations for the X $^3A_2'$ state of TMM, which use three active unoccupied orbitals to select the dominant 3p-1h and 4p-2h amplitudes, are approximately twice as fast as the corresponding DEA-EOMCC(4p-2h)$\{N_u\}$ computations, in which 3p-1h contributions are treated fully. At the same time, as shown in the next section, there is virtually no loss of accuracy when the singlet−triplet gaps in TMM resulting from the DEA-EOMCC(3p-1h,4p-2h)$\{3\}$ and DEA-EOMCC(4p-2h)$\{3\}$ calculations are compared with each other and with experiment.

Interestingly, the CPU timings of the higher-level DEA-EOMCC(3p-1h,4p-2h)$\{3\}$ calculations for the TMM system, which include 3p-1h and 4p-2h contributions, are on the same order as the timings characterizing the corresponding lower-level DEA-EOMCC(3p-1h) computations, which neglect 4p-2h effects altogether. This is especially true when the larger cc-pVTZ basis set is employed. We observe the same when other molecular systems are examined. Thus, with the development of the DEA-EOMCC(3p-1h,4p-2h)$\{N_u\}$ method in this work, we gained the ability to perform routine calculations at the very high DEA-EOMCC(4p-2h) level, at least for the medium-size molecular systems, which, as shown in the next section and our earlier work,[51,52] provide chemical (∼1 kcal/mol) or better accuracy in describing low-lying states of biradicals and single bond breaking in closed-shell species, improving the results of the corresponding DEA-EOMCC(3p-1h) calculations. At the same time, through the development of the active-space DEA-EOMCC(3p-1h)$\{N_u\}$ approach in this study, we made the DEA-EOMCC(3p-1h) calculations a lot more practical. For example, as shown in Table 1, the DEA-EOMCC(3p-1h)$\{3\}$ calculations for TMM are ∼30 times faster than the corresponding full DEA-EOMCC(3p-1h) computations, when the cc-pVTZ basis set is employed, and, as demonstrated in the next section, there is virtually no loss of accuracy in the description of the singlet−triplet gap in TMM when full DEA-EOMCC(3p-1h) is replaced by its active-space DEA-EOMCC-(3p-1h)$\{N_u\}$ counterpart.

3. NUMERICAL EXAMPLES

To assess the performance of the active-space DEA-EOMCC-(3p-1h)$\{N_u\}$ and DEA-EOMCC(3p-1h,4p-2h)$\{N_u\}$ methods, we performed several benchmark calculations that are representative of the types of problems such methods may be useful for, which are low-lying singlet and triplet states of biradical species and single bond breaking in closed-shell molecules leading to doublet radical fragments. We compare the results obtained in the DEA-EOMCC(3p-1h)$\{N_u\}$ and DEA-EOMCC(3p-1h,4p-2h)$\{N_u\}$ calculations, in which 3p-1h or 3p-1h and 4p-2h components of $R_\mu^{(+2)}$ are treated using active orbitals, with the parent full DEA-EOMCC(3p-1h) and DEA-EOMCC(4p-2h) data and the results of the DEA-EOMCC(4p-2h)$\{N_u\}$ computations, in which 4p-2h amplitudes are selected using active orbitals, but 3p-1h contributions are treated fully. Some of the benchmark systems discussed in this section are small enough to allow for the exact, full CI, and nearly exact, full DEA-EOMCC(4p-2h) calculations, and all of them can be treated with the DEA-EOMCC(3p-1h) and DEA-EOMCC(4p-2h)$\{N_u\}$ approaches that provide useful reference data for their less expensive DEA-EOMCC(3p-1h)$\{N_u\}$ and DEA-EOMCC(3p-1h,4p-2h)$\{N_u\}$ counterparts.

We examine the following molecular problems: (i) the adiabatic energy gaps between the triplet ground state (X $^3B_1$) and the three low-lying singlet excited states (A $^1A_1$, B $^1B_1$, and C $^1A_1$) of methylene, as described by the [5s3p/3s] triple-ζ basis set of Dunning[85] augmented with two sets of polarization functions, abbreviated as TZ2P, for which the exact, full CI,

DOI: 10.1021/acs.jpca.6b11393
J. Phys. Chem. A 2017, 121, 3469−3485

Table 2. A Comparison of the Full CI and Various DEA-EOMCC Adiabatic Excitation Energies, along with the Corresponding MUE and NPE Values Relative to Full CI, Characterizing the Low-Lying States of Methylene, as Described by the TZ2P Basis Set[a]

orbitals	method	A $^1A_1$ − X $^3B_1$	B $^1B_1$ − X $^3B_1$	C $^1A_1$ − X $^3B_1$	MUE	NPE
(N − 2)-electron RHF[b]	DEA-EOMCC(3p-1h){2}[c]	1.30	−0.82	−1.00	1.30	2.30
	DEA-EOMCC(3p-1h)	−0.11	−1.89	−3.64	3.64	3.53
	DEA-EOMCC(3p-1h,4p-2h){2}[c]	1.67	0.82	2.28	2.28	1.46
	DEA-EOMCC(4p-2h){2}[c]	0.13	−0.35	−0.54	0.54	0.67
	DEA-EOMCC(4p-2h)	0.38	−0.02	0.21	0.38	0.40
N-electron ROHF[d]	DEA-EOMCC(3p-1h){2}[c]	1.47	0.63	1.42	1.47	0.84
	DEA-EOMCC(3p-1h)	0.64	0.10	0.45	0.64	0.54
	DEA-EOMCC(3p-1h,4p-2h){2}[c]	0.63	0.48	0.58	0.63	0.16
	DEA-EOMCC(4p-2h){2}[c]	−0.22	−0.05	−0.29	0.29	0.24
	DEA-EOMCC(4p-2h)	0.19	0.08	0.37	0.37	0.29
N-electron RHF[e]	DEA-EOMCC(3p-1h){2}[c]	−0.11	−0.50	0.17	0.50	0.67
	DEA-EOMCC(3p-1h)	0.29	−0.15	−0.31	0.31	0.60
	DEA-EOMCC(3p-1h,4p-2h){2}[c]	0.16	−0.42	−0.01	0.42	0.60
	DEA-EOMCC(4p-2h){2}[c]	0.66	−0.02	−0.28	0.66	0.94
	DEA-EOMCC(4p-2h)	0.14	0.09	0.38	0.38	0.29
N-electron ROHF/RHF[f]	DEA-EOMCC(3p-1h){2}[c]	2.19	1.79	2.46	2.46	0.67
	DEA-EOMCC(3p-1h)	1.53	1.09	0.93	1.53	0.60
	DEA-EOMCC(3p-1h,4p-2h){2}[c]	0.76	0.18	0.59	0.76	0.58
	DEA-EOMCC(4p-2h){2}[c]	0.12	−0.56	−0.82	0.82	0.94
	DEA-EOMCC(4p-2h)	0.19	0.14	0.43	0.43	0.29
	full CI[a]	11.14	35.59	61.67		

[a]The basis set, geometries, and full CI energies were taken from ref 86. The full CI values are the adiabatic excitation energies (in kcal/mol), whereas the remaining values are errors relative to full CI (also in kcal/mol). The CH_2^{2+} reference system used in the DEA-EOMCC calculations was created by vacating the $3a_1$ HOMO of CH_2. As in ref 86, the lowest occupied orbital and the highest unoccupied orbital were frozen in the post-SCF calculations and the spherical components of the carbon d orbital were employed throughout. [b]The DEA-EOMCC calculations using the RHF orbitals obtained for the singlet ground state of CH_2^{2+}. [c]The active space consisted of the HOMO and LUMO of CH_2, $3a_1$ and $1b_1$, respectively, which are unoccupied in the CH_2^{2+} reference system used in the DEA-EOMCC calculations. [d]The DEA-EOMCC calculations using the ROHF orbitals obtained for the X $^3B_1$ state of CH_2. [e]The DEA-EOMCC calculations using the RHF orbitals obtained for the A $^1A_1$ state of CH_2. [f]The DEA-EOMCC calculations using the ROHF orbitals of CH_2 for the X $^3B_1$ state and the A $^1A_1$ RHF orbitals of CH_2 for the remaining three states.

results have been reported in ref 86 (see Tables 2 and 3), (ii) the adiabatic separation between the D_{3h}-symmetric X $^3A_2'$ ground state, which has a largely single-reference nature, and the C_{2v}-symmetric B $^1A_1$ excited state, which has a multireference, biradical character, in TMM, as described by the cc-pVDZ and cc-pVTZ basis sets, which has accurately been determined in ref 87 by subtracting the theoretical zero-point vibrational energy corrections (ΔZPVE) resulting from the spin-flip density functional theory (SF-DFT/6-31G(d)) calculations[87] from the experimental values of the B $^1A_1$ − X $^3A_2'$ gap obtained in photoelectron spectroscopy measurements in ref 88 (see Table 4; cf. Table 1 for the corresponding CPU timings), (iii) the vertical singlet−triplet gaps in the antiaromatic CBD (C_4H_4) and CPC [$(C_5H_5)^+$] biradicals, as described by the cc-pVDZ basis set, assuming the D_{4h}-symmetric (CBD) and D_{5h}-symmetric (CPC) geometries of the corresponding triplet states optimized in ref 89 (see Table 5), and (iv) the F−F bond dissociation in the F_2 molecule, as described by the double-ζ (DZ) basis set,[90] for which the exact, full CI, results can be found in ref 91 (see Table 6). In the methylene and F_2 examples, where our DEA-EOMCC data are compared with the corresponding full CI results, in addition to the individual errors for the various energy gaps (methylene) or electronic energies at different nuclear geometries (F_2), we provide information about the corresponding maximum unsigned error (MUE) and nonparallelity error (NPE) values relative to full CI (see Tables 2, 3, and 6). In the case of the adiabatic energy gaps in methylene obtained in the various DEA-EOMCC calculations (Table 2), we compare them with the corresponding CI computations, where we diagonalize the bare Hamiltonian instead of the similarity-transformed Hamiltonian in the same spaces as those used in the DEA-EOMCC diagonalizations (Table 3), to illustrate the point that diagonalizing $\bar{H}$ instead of H greatly benefits the resulting energetics. Also, our description of the adiabatic B $^1A_1$ − X $^3A_2'$ gap in TMM at the DEA-EOMCC(3p-1h) and DEA-EOMCC(4p-2h){N_u} levels, which provide reference data for the considerably less demanding DEA-EOMCC(3p-1h){N_u} and DEA-EOMCC(3p-1h,4p-2h){N_u} calculations, is enriched by reporting the results obtained with the larger cc-pVTZ basis sets, in addition to the cc-pVDZ basis set used in refs 51 and 52 (see Table 4).

One of the important aspects of any DEA-EOMCC work is the choice of orbitals used to construct the corresponding wave function expansions. Thus, in analogy to refs 51 and 52 (see also refs 47 and 48), we examine this aspect here as well. As explained in refs 51 and 52, one typically has a choice between the symmetry-adapted RHF or ROHF orbitals obtained in the calculations for the singlet (RHF) and triplet (ROHF) states of the N-electron target system or the RHF MOs optimized for the corresponding (N − 2)-electron closed-shell core. Both strategies are considered in this work. In doing so, one must be aware of the fact that the singlet RHF orbitals of the target N-electron system may lift orbital degeneracies when the N-electron species of interest has a non-Abelian symmetry, resulting in the undesirable symmetry-broken DEA-EOMCC wave function expansions.[51,52] As further elaborated on below, this would, for example, happen if we tried to exploit the RHF MOs optimized for the B $^1A_1$ singlet state of TMM in the

DOI: 10.1021/acs.jpca.6b11393
J. Phys. Chem. A 2017, 121, 3469−3485

Table 3. A Comparison of the Full CI and Various CI(np-(n−2)h), where n > 2, Adiabatic Excitation Energies, along with the Corresponding MUE and NPE Values Relative to Full CI, Characterizing the Low-Lying States of Methylene, as Described by the TZ2P Basis Set[a]

orbitals	method	A $^1A_1$ − X $^3B_1$	B $^1B_1$ − X $^3B_1$	C $^1A_1$ − X $^3B_1$	MUE	NPE
(N − 2)-electron RHF[b]	CI(3p-1h){2}[c]	3.00	0.43	7.31	7.31	6.88
	CI(3p-1h)	1.40	−0.72	4.12	4.12	4.84
	CI(3p-1h,4p-2h){2}[c]	4.17	2.25	11.26	11.26	9.01
	CI(4p-2h){2}[c]	2.42	0.96	7.75	7.75	6.79
	CI(4p-2h)	2.73	1.38	8.57	8.57	7.19
N-electron ROHF[d]	CI(3p-1h){2}[c]	7.79	6.73	10.14	10.14	3.40
	CI(3p-1h)	7.44	6.49	9.70	9.70	3.21
	CI(3p-1h,4p-2h){2}[c]	9.29	5.96	8.11	9.29	3.33
	CI(4p-2h){2}[c]	9.14	5.85	8.03	9.14	3.29
	CI(4p-2h)	8.94	5.10	7.58	8.94	3.84
N-electron RHF[e]	CI(3p-1h){2}[c]	6.21	4.08	11.68	11.68	7.60
	CI(3p-1h)	7.95	4.77	11.32	11.32	6.54
	CI(3p-1h,4p-2h){2}[c]	9.80	4.04	11.36	11.36	7.32
	CI(4p-2h){2}[c]	11.93	4.89	11.58	11.58	7.03
	CI(4p-2h)	10.14	4.65	11.38	11.38	6.74
N-electron ROHF/RHF[f]	CI(3p-1h){2}[c]	1.42	−0.71	6.89	6.89	7.60
	CI(3p-1h)	0.69	−2.49	4.05	4.05	6.54
	CI(3p-1h,4p-2h){2}[c]	0.53	−5.24	2.08	5.24	7.32
	CI(4p-2h){2}[c]	−0.07	−7.10	−0.41	7.10	7.03
	CI(4p-2h)	−0.34	−5.83	0.91	5.83	6.74
	full CI[a]	11.14	35.59	61.67		

[a]The basis set, geometries, and full CI energies were taken from ref 86. The full CI values are the adiabatic excitation energies (in kcal/mol), whereas the remaining values are errors relative to full CI (also in kcal/mol). The CH_2^{2+} reference system used in the CI(np-(n−2)h) calculations was created by vacating the $3a_1$ HOMO of CH_2. As in ref 86, the lowest occupied orbital and the highest unoccupied orbital were frozen in the post-SCF calculations and the spherical components of the carbon d orbital were employed throughout. [b]The CI(np-(n−2)h) calculations using the RHF orbitals obtained for the singlet ground state of CH_2^{2+}. [c]The active space consisted of the HOMO and LUMO of CH_2, $3a_1$ and $1b_1$, respectively, which are unoccupied in the CH_2^{2+} reference system used in the CI(np-(n−2)h) calculations. [d]The CI(np-(n−2)h) calculations using the ROHF orbitals obtained for the X $^3B_1$ state of CH_2. [e]The CI(np-(n−2)h) calculations using the RHF orbitals obtained for the A $^1A_1$ state of CH_2. [f]The CI(np-(n−2)h) calculations using the ROHF orbitals of CH_2 for the X $^3B_1$ state and the A $^1A_1$ RHF orbitals of CH_2 for the remaining three states.

Table 4. Selected DEA-EOMCC Results for the Adiabatic Singlet−Triplet Separation $\Delta E_{S-T} = E(B\ ^1A_1) - E(X\ ^3A_2')$ (in kcal/mol) in Trimethylenemethane, as Described by the cc-pVDZ and, in Parentheses, cc-pVTZ Basis Sets, Calculated Using the SF-DFT/6-31G(d) Geometries Obtained in Ref 87[a]

	orbitals		
method	(N − 2)-electron RHF[b]	N-electron ROHF[c]	N-electron ROHF/RHF[d]
DEA-EOMCC(3p-1h){3}[e]	24.2 (24.0)	19.6 (22.3)	21.5 (22.3)
DEA-EOMCC(3p-1h)	23.9 (23.5)	19.4 (21.1)	20.9 (21.1)
DEA-EOMCC(3p-1h,4p-2h){3}[e]	19.3 (18.9)	18.7 (19.9)	19.4 (19.9)
DEA-EOMCC(4p-2h){3}[e]	19.0 (18.4)	18.6 (18.7)	18.9 (18.7)
expt[f]		16.1 ± 0.1	
expt − ΔZPVE[g]		18.1	

[a]The TMM^{2+} reference system used in the DEA-EOMCC calculations was created by vacating the doubly degenerate valence 1e″ (the D_{3h}-symmetric X $^3A_2'$ state) or nondegenerate $1a_2$ and $2b_1$ (the C_{2v}-symmetric B $^1A_1$ state) orbitals of the TMM's π system. The lowest-energy core orbitals correlating with the 1s shells of the carbon atoms were frozen in the post-SCF calculations and the spherical components of the d and f orbitals were employed throughout. [b]The DEA-EOMCC calculations using the RHF orbitals of the singlet ground state of TMM^{2+}. [c]The DEA-EOMCC calculations using the ROHF orbitals obtained for the triplet ground state of TMM. [d]The DEA-EOMCC calculations using the ROHF orbitals of TMM for the X $^3A_2'$ state and the RHF orbitals of TMM for the B $^1A_1$ state. [e]The active space consisted of the doubly degenerate 1e″ and nondegenerate $2a_2''$ orbitals (using the D_{3h} symmetry of the X $^3A_2'$ state) or the $1a_2$, $2b_1$, and $3b_1$ orbitals (using the C_{2v} symmetry of the B $^1A_1$ state), which are the three lowest-energy unoccupied MOs in the TMM^{2+} reference system. [f]From ref 88. [g]The estimate of the purely electronic ΔE_{S-T} gap obtained by subtracting the zero-point vibrational energy corrections, ΔZPVE, resulting from the SF-DFT/6-31G(d) calculations reported in ref 87 from the experimental singlet−triplet separation determined in ref 88.

calculations for the corresponding D_{3h}-symmetric X $^3A_2'$ triplet state. In cases like this, one can either use the high-spin ROHF orbitals of the N-electron target system or the dicationic RHF orbitals corresponding to the (N − 2)-electron closed-shell core, which allow us to maintain the relevant spatial symmetries throughout the DEA-EOMCC calculations (adaptation to spin symmetry is automatic as long as restricted orbitals are employed). This is what we do in this work, that is, all of the DEA-EOMCC calculations discussed in this paper provide spin- and symmetry-adapted results. One of the main findings of our previous studies,[51,52] especially those reported in ref 52, was the observation that the results of the DEA-EOMCC

DOI: 10.1021/acs.jpca.6b11393
J. Phys. Chem. A 2017, 121, 3469−3485

Table 5. Selected DEA-EOMCC Results for the Vertical Singlet−Triplet Gaps, $\Delta E_{S-T} = E(S) - E(T)$ (in kcal/mol), in the Cyclobutadiene C_4H_4 System (CBD) and the Cyclopentadienyl $(C_5H_5)^+$ Cation (CPC), as Described by the cc-pVDZ Basis Set, Calculated at the Corresponding D_{4h}-Symmetric (CBD) and D_{5h}-Symmetric (CPC) Triplet Geometries Optimized in Ref 89[a]

method	CBD	CPC
DEA-EOMCC(3p-1h){N_u}	−1.37[b]	16.38[c]
DEA-EOMCC(3p-1h)	−1.42	16.06
DEA-EOMCC(3p-1h,4p-2h){N_u}	−4.98[b]	14.25[c]
DEA-EOMCC(4p-2h){N_u}	−5.04[b]	13.91[c]

[a]The CBD^{2+} and CPC^{2+} reference systems used in the DEA-EOMCC calculations were created by vacating the doubly degenerate valence π orbitals of the CBD and CPC molecules, respectively (i.e., the highest singly occupied MOs of $e_g(D_{4h})$ symmetry in the triplet CBD species and the highest singly occupied MOs of $e_1''(D_{5h})$ symmetry in the triplet CPC species). The lowest-energy core orbitals correlating with the 1s shells of the carbon atoms were frozen in the post-SCF calculations and the spherical components of the d orbitals were employed throughout. All DEA-EOMCC calculations were performed using the RHF MOs optimized for the CBD^{2+} and CPC^{2+} reference systems. [b]The active space consisted of the $N_u = 3$ lowest-energy unoccupied π MOs in the CBD^{2+} system, including the doubly degenerate $e_g(D_{4h})$ orbital, which was vacated when forming CBD^{2+} from CBD, and the nondegenerate $b_{2u}(D_{4h})$ orbital, which is empty in CBD^{2+} and CBD. [c]The active space consisted of the $N_u = 4$ lowest-energy unoccupied π MOs in the CPC^{2+} system, including the doubly degenerate $e_1''(D_{5h})$ orbital, which was vacated when forming CPC^{2+} from CPC, and the doubly degenerate $e_2''(D_{5h})$ orbital, which is empty in CPC^{2+} and CPC.

computations including 4p-2h contributions are practically insensitive to the choice of the underlying MO basis, whereas their lower-order DEA-EOMCC(3p-1h) counterparts may display a significant dependence on the type of orbitals used in the calculations. A similar behavior is observed in this work; that is, the results obtained with the active-space DEA-EOMCC(3p-1h,4p-2h){N_u} approach are not only in very good agreement with the corresponding DEA-EOMCC(4p-2h){N_u} and DEA-EOMCC(4p-2h) data, especially if we take into account the relatively low costs of the DEA-EOMCC(3p-1h,4p-2h){N_u} calculations, but they are also less sensitive to the choice of the underlying MO basis than the corresponding DEA-EOMCC(3p-1h){N_u} and DEA-EOMCC(3p-1h) results. At the same time, the results of the active-space DEA-EOMCC(3p-1h){N_u} calculations display a similar dependence on the underlying MO basis as their parent DEA-EOMCC(3p-1h) counterparts.

3.1. Adiabatic Energy Gaps Involving Low-Lying Singlet and Triplet States of Methylene. We begin our discussion with the various DEA-EOMCC results for the X $^3B_1$, A $^1A_1$, B $^1B_1$, and C $^1A_1$ electronic states of methylene, as described by the TZ2P basis set used in ref 86, where the authors performed the corresponding full CI calculations, optimizing the geometry of each of the four states at the full CI level as well. In performing the DEA-EOMCC calculations with the full and active-space treatments of 3p-1h and 4p-2h excitations, summarized in Table 2, and the analogous CI calculations, in which the diagonalization of the similarity-transformed Hamiltonian of CCSD was replaced by the diagonalization of the bare Hamiltonian, summarized in Table 3, we adopted the full CI/TZ2P geometries of the X $^3B_1$, A $^1A_1$, B $^1B_1$, and C $^1A_1$ states reported in ref 86. We focus on the adiabatic energy gaps between the triplet ground state and the three lowest-energy singlet excited states.

Let us recall that a few decades ago methylene was the subject of serious controversies between theory and experiment concerning the geometry of its triplet ground state and the small energy gap between the X $^3B_1$ and A $^1A_1$ states, where theory turned out to be crucial for providing correct answers (cf. refs 92−97 for selected historical accounts). Because of its small size, which allows for all kinds of electronic structure calculations, and because of its complicated electronic spectrum, which consists of excited states that are difficult to describe in an accurate and balanced manner, methylene has become an important benchmark system for testing quantum chemistry methods (cf. refs 51 and 52 and a long list of papers cited therein for some of the most representative examples of the past ab initio computations for CH_2). We also recall that, while the ground and second excited states, X $^3B_1$ and B $^1B_1$, respectively, can be characterized as having a single-reference character, which is well represented by the high-spin triplet and open-shell singlet configurations of the $(1a_1)^2(2a_1)^2(1b_2)^2(3a_1)^1(1b_1)^1$ type, the first excited A $^1A_1$ state and the third excited C $^1A_1$ state have a manifestly multireference nature that originates from mixing the $(1a_1)^2(2a_1)^2(1b_2)^2(3a_1)^2$ and $(1a_1)^2(2a_1)^2(1b_2)^2(1b_1)^2$ configurations, which is particularly severe in the case of the strongly biradical C $^1A_1$ state. Thus, to obtain accurate results for the adiabatic energy gaps between the X $^3B_1$ ground state and the A $^1A_1$, B $^1B_1$, and C $^1A_1$

Table 6. A Comparison of the Full CI and Various DEA-EOMCC Ground-State Energies of F_2 at the Equilibrium (R_e = 2.668 16 bohr) and a Few Other F−F Distances, along with the Corresponding MUE and NPE Values Relative to Full CI, Obtained with the DZ Basis Set[a]

method	R_e	$1.1R_e$	$1.2R_e$	$1.5R_e$	$2R_e$	$3R_e$	$4R_e$	MUE	NPE
DEA-EOMCC(3p-1h){2}[b]	−3.538	−2.808	−2.210	1.585	1.860	1.360	1.279	3.538	5.398
DEA-EOMCC(3p-1h)	−3.947	−3.181	−2.563	1.305	1.485	1.015	0.935	3.947	5.432
DEA-EOMCC(3p-1h,4p-2h){2}[b]	3.807	3.508	3.193	1.665	1.895	1.656	1.601	3.807	2.206
DEA-EOMCC(4p-2h){2}[b]	3.437	3.161	2.855	1.371	1.505	1.298	1.244	3.437	2.193
DEA-EOMCC(4p-2h)	2.314	2.195	2.061	0.628	0.807	0.762	0.720	2.314	1.686
full CI[a]	0.968 128	0.976 458	0.972 125	0.952 558	0.945 201	0.944 819	0.944 831		

[a]The full CI values are total energies E, taken from ref 91, reported as $-(E + 198)$ Ha. The remaining energies are errors relative to full CI, in millihartree (mHa). The F_2^{2+} reference system used in the DEA-EOMCC calculations was created by vacating the valence σ_g orbital of F_2. Following ref 91, the RHF orbitals of F_2 were employed throughout and the two lowest-energy core orbitals and the corresponding two highest-energy unoccupied orbitals were frozen in the post-SCF calculations. [b]The active space consisted of the valence σ_g and σ_u orbitals, which are unoccupied in the F_2^{2+} reference system utilized in the DEA-EOMCC calculations.

DOI: 10.1021/acs.jpca.6b11393
J. Phys. Chem. A 2017, 121, 3469−3485

excited states, one must use methods that can provide a well-balanced treatment of the dynamical and nondynamical electron correlation effects. This makes methylene a valuable benchmark system for testing the active-space DEA-EOMCC-(3p-1h)$\{N_u\}$ and DEA-EOMCC(3p-1h,4p-2h)$\{N_u\}$ methods developed in this work.

In all of the DEA-EOMCC calculations summarized in Table 2, the $(N-2)$-electron CH_2^{2+} reference system was obtained by vacating the highest occupied MO (HOMO), $3a_1$, of CH_2. To examine the dependence of the various DEA-EOMCC results on the type of orbitals that are used to define the corresponding wave function expansions, we used both the ground-state RHF orbitals of the CH_2^{2+} reference dication and the RHF or ROHF MOs optimized for the CH_2 target system. In the latter case, we followed refs 51 and 52 and adopted three different strategies. In the first strategy, we constructed the DEA-EOMCC wave function expansions for all the calculated states using the ROHF orbitals obtained for the X $^3B_1$ state of methylene. In the second strategy, we utilized the RHF orbitals optimized for the A $^1A_1$ state. In the third strategy, we used the X $^3B_1$ ROHF orbitals in the DEA-EOMCC calculations for the triplet ground state and the A $^1A_1$ RHF orbitals for the remaining three singlet states. For each choice of the MO basis, the active orbitals employed in the DEA-EOMCC(3p-1h)$\{N_u\}$, DEA-EOMCC-(3p-1h,4p-2h)$\{N_u\}$, and DEA-EOMCC(4p-2h)$\{N_u\}$ calculations were the HOMO orbital $3a_1$ and the lowest unoccupied MO (LUMO) $1b_1$ of methylene, which are unoccupied in the CH_2^{2+} dication that serves as a reference system for the DEA-EOMCC considerations. In other words, the number of active unoccupied orbitals N_u, used to define 3p-1h component in the DEA-EOMCC(3p-1h)$\{N_u\}$ calculations, 3p-1h and 4p-2h components in the DEA-EOMCC(3p-1h,4p-2h)$\{N_u\}$ computations, and 4p-2h component in the DEA-EOMCC(4p-2h)$\{N_u\}$ calculations, was set at 2, making the resulting diagonalizations of the similarity-transformed Hamiltonian only a few times more expensive than the conventional closed-shell CCSD calculations in the DEA-EOMCC(3p-1h,4p-2h)$\{N_u\}$ and DEA-EOMCC(4p-2h)$\{N_u\}$ cases and less expensive than CCSD in the case of DEA-EOMCC(3p-1h)$\{N_u\}$. As shown in ref 51, the DEA-EOMCC(4p-2h)$\{2\}$ calculations for the TZ2P model of methylene considered here are ~400 times faster than the corresponding full DEA-EOMCC(4p-2h) computations and only 4 times slower than the DEA-EOMCC(3p-1h) calculations. The DEA-EOMCC(3p-1h,4p-2h)$\{2\}$ computations are even faster.

The adiabatic A $^1A_1$ − X $^3B_1$, B $^1B_1$ − X $^3B_1$, and C $^1A_1$ − X $^3B_1$ excitation energies collected in Table 2 and the corresponding MUE and NPE values demonstrate that there is a generally good agreement between the results of the inexpensive active-space DEA-EOMCC(3p-1h)$\{2\}$ calculations and their full DEA-EOMCC(3p-1h) counterparts and among the results of the active-space DEA-EOMCC(3p-1h,4p-2h)$\{2\}$ and DEA-EOMCC(4p-2h)$\{2\}$ and full DEA-EOMCC(4p-2h) computations. As opposed to the DIP-EOMCC approach truncated at 3h-1p excitations, which we examined in our previous studies[51,52] and which in the case of the TZ2P model of methylene may produce errors as large as 10.94 kcal/mol, none of the DEA-EOMCC methods examined in the present work fails; that is, the DEA-EOMCC calculations truncated at 3p-1h terms are capable of providing reasonable gap values, especially when one uses MOs optimized for the target CH_2 system. Nevertheless, the inclusion of 4p-2h correlations through the relatively inexpensive DEA-EOMCC-(3p-1h,4p-2h)$\{2\}$ calculations, which describe 3p-1h and 4p-2h effects using active orbitals, is helpful and worth analyzing here.

We first observe that the differences between the DEA-EOMCC(3p-1h)$\{2\}$ and DEA-EOMCC(3p-1h) gap values are almost identical to the analogous differences between the gaps obtained in the DEA-EOMCC(3p-1h,4p-2h)$\{2\}$ and DEA-EOMCC(4p-2h)$\{2\}$ calculations. Indeed, if we, for example, examine the A $^1A_1$ − X $^3B_1$ energy separations calculated using the RHF MOs of the CH_2^{2+} reference system, the ROHF MOs optimized for the triplet ground state of CH_2, the RHF MOs optimized for the A $^1A_1$ state of CH_2, and the ROHF MOs of CH_2 for the X $^3B_1$ state combined with the RHF MOs of CH_2 for the singlet states, the differences between the DEA-EOMCC(3p-1h)$\{2\}$ and DEA-EOMCC(3p-1h) results, of 1.41, 0.83, 0.40, and 0.66 kcal/mol, respectively, are almost identical to the analogous differences between the DEA-EOMCC(3p-1h,4p-2h)$\{2\}$ and DEA-EOMCC(4p-2h)$\{2\}$ data, which are 1.54, 0.85, 0.50, and 0.64 kcal/mol. This is not surprising, since the DEA-EOMCC(3p-1h)$\{2\}$ and DEA-EOMCC(3p-1h) calculations and the DEA-EOMCC(3p-1h,4p-2h)$\{2\}$ and DEA-EOMCC(4p-2h)$\{2\}$ calculations differ in exactly the same manner, namely, DEA-EOMCC(3p-1h)$\{2\}$ and DEA-EOMCC(3p-1h,4p-2h)$\{2\}$ treat 3p-1h terms using active orbitals, whereas DEA-EOMCC(3p-1h) and DEA-EOMCC(4p-2h)$\{2\}$ treat them fully. Because of the approximate treatment of 3p-1h contributions in the DEA-EOMCC-(3p-1h,4p-2h)$\{2\}$ calculations, the agreement between the DEA-EOMCC(3p-1h,4p-2h)$\{2\}$ and full DEA-EOMCC-(4p-2h) data is not as good as in the case of DEA-EOMCC-(4p-2h)$\{2\}$, which uses active orbitals to select the higher-rank 4p-2h excitations, while treating 3p-1h contributions fully, but the relatively inexpensive DEA-EOMCC(3p-1h,4p-2h)$\{2\}$ calculations, which capture the dominant 3p-1h and 4p-2h correlations, improve the DEA-EOMCC(3p-1h)$\{2\}$ and DEA-EOMCC(3p-1h) results that neglect 4p-2h physics altogether. For example, if we look at the largest unsigned errors relative to full CI obtained in the calculations of the adiabatic A $^1A_1$ − X $^3B_1$, B $^1B_1$ − X $^3B_1$, and C $^1A_1$ − X $^3B_1$ energy gaps, represented in Table 2 by the MUE values, and focus on the DEA-EOMCC results obtained using the ROHF MOs of CH_2 for the triplet ground state and the RHF MOs of CH_2 for the remaining three singlet states, we can see significant improvement when going from DEA-EOMCC(3p-1h)$\{2\}$ and DEA-EOMCC(3p-1h), which give MUEs of 2.46 and 1.53 kcal/mol, respectively, to DEA-EOMCC(3p-1h,4p-2h)$\{2\}$, which gives MUE of 0.76 kcal/mol. In fact, the MUE value characterizing the DEA-EOMCC(3p-1h,4p-2h)$\{2\}$ calculations is virtually identical to that obtained with the more expensive DEA-EOMCC(4p-2h)$\{2\}$ approach, which gives 0.82 kcal/mol, and not much worse than the MUE of 0.43 kcal/mol characterizing the corresponding full DEA-EOMCC(4p-2h) computations. When the ROHF MOs of CH_2 are used in the calculations for all four states, the largest errors obtained with the active-space DEA-EOMCC(3p-1h,4p-2h)$\{2\}$ and full DEA-EOMCC-(3p-1h) approaches are virtually identical, but the NPE characterizing the DEA-EOMCC(3p-1h,4p-2h)$\{2\}$ data, of 0.16 kcal/mol, is more than 3 times smaller than the NPE characterizing the corresponding DEA-EOMCC(3p-1h) results (0.54 kcal/mol). The use of MOs obtained in the RHF calculations for the CH_2^{2+} dication worsens the DEA-EOMCC-(3p-1h,4p-2h)$\{2\}$ results somewhat, but they are still better than the results of the corresponding DEA-EOMCC(3p-1h)

DOI: 10.1021/acs.jpca.6b11393
J. Phys. Chem. A 2017, 121, 3469−3485

computations, reducing the MUE and NPE values characterizing the adiabatic A $^1A_1$ − X $^3B_1$, B $^1B_1$ − X $^3B_1$, and C $^1A_1$ − X $^3B_1$ separations by 1.36 and 2.07 kcal/mol, respectively.

Consistent with our earlier work,[52] we observe a smaller dependence of the A $^1A_1$ − X $^3B_1$, B $^1B_1$ − X $^3B_1$, and C $^1A_1$ − X $^3B_1$ gaps obtained with the DEA-EOMCC(3p-1h,4p-2h){2}, DEA-EOMCC(4p-2h){2}, and DEA-EOMCC(4p-2h) approaches on the orbitals used in the calculations than that observed when the lower-order DEA-EOMCC(3p-1h){2} and DEA-EOMCC(3p-1h) methods, neglecting 4p-2h contributions, are employed. Indeed, if we look at the numerical data listed in Table 2, we can see that the ranges of the NPE values characterizing the DEA-EOMCC(3p-1h){2} and DEA-EOMCC(3p-1h) results, when all types of MOs are included in the analysis, are 0.67−2.30 and 0.54−3.53 kcal/mol, respectively. The DEA-EOMCC(3p-1h,4p-2h){2}, DEA-EOMCC(4p-2h){2}, and DEA-EOMCC(4p-2h) calculations reduce these ranges to 0.16−1.46, 0.24−0.94, and 0.29−0.40 kcal/mol, respectively. This can be understood if we realize that by incorporating 4p-2h components in the DEA-EOMCC diagonalizations we bring the results closer to the orbital-invariant exact, full CI, limit, in which all $R_{\mu,np\text{-}(n-2)h}$ components with n = 2, ..., N are included in $R_\mu^{(+2)}$. As one might expect, the largest singly excited (T_1) cluster amplitudes obtained in the underlying CCSD calculations for the CH_2^{2+} reference dication increase in absolute value when the $(N-2)$-electron MO basis optimized for CH_2^{2+} is replaced by one of the N-electron bases optimized for CH_2, from a 0.01−0.02 level, when the RHF MOs determined for CH_2^{2+} are employed, to ∼0.13−0.17, when the RHF/ROHF orbitals optimized for CH_2 are adopted, but this is not a key factor in the understanding orbital dependence or the lack thereof in the case of the DEA-EOMCC results shown in Table 2. By the virtue of the presence of the Thouless-like e^{T_1} factor in the CCSD wave function, the CCSD calculations for CH_2^{2+} can absorb orbital rotations that result in T_1 amplitudes on the order of 0.1−0.2. What is the key is the neglect or the incorporation of the higher many-body components of the $R_\mu^{(+2)}$ operator in the DEA-EOMCC diagonalizations. The inclusion of the higher-order 4p-2h components, fully, as in the DEA-EOMCC(4p-2h) approach, or approximately, as in the active-space DEA-EOMCC(4p-2h){N_u} and DEA-EOMCC(3p-1h,4p-2h){N_u} schemes, makes the resulting excitation energies less sensitive to the MO basis employed in the calculations. Clearly, the DEA-EOMCC(3p-1h,4p-2h){2} computations, in which both 3p-1h and 4p-2h components are treated approximately using a small number of active MOs, have a larger sensitivity to the underlying MO basis than the corresponding DEA-EOMCC-(4p-2h){2} and DEA-EOMCC(4p-2h) calculations, but the variation in the NPE values characterizing the DEA-EOMCC-(3p-1h,4p-2h){2} results, of 0.16−1.46 kcal/mol, remains relatively small, being acceptable in many applications. Interestingly, the variation in the NPE values characterizing the DEA-EOMCC(3p-1h,4p-2h){2} calculations becomes even smaller when we exclude the results obtained with the MOs optimized for the CH_2^{2+} dication. When we do this, the range of the NPE values characterizing the DEA-EOMCC(3p-1h,4p-2h){2} results reduces to 0.16−0.60 kcal/mol (a similarly small error range, 0.42−0.76 kcal/mol, is obtained when examining the corresponding MUE data). When the data obtained with the ionic MOs are ignored, the active-space DEA-EOMCC(3p-1h,4p-2h){2} approach becomes competitive with its more expensive DEA-EOMCC-(4p-2h){2} counterpart, which produces the NPE and MUE ranges of 0.24−0.94 and 0.29−0.82 kcal/mol, respectively.

It is well known that the diagonalization of the similarity-transformed Hamiltonian of CC theory exploited in EOMCC considerations offers substantial improvements in the results over the analogous CI diagonalizations of the bare Hamiltonian. As pointed out in Section 2.1, the latter diagonalizations also violate important formal conditions, such as the requirement of size intensivity of the resulting excitation, electron attachment, and ionization energies. We already discussed the relative performance of $\bar{H}$ versus H diagonalizations in the context of the EA/IP EOMCC calculations through 4p-3h/4h-3p excitations in ref 43, demonstrating that the diagonalizations of $\bar{H}$ are a lot more effective than the corresponding diagonalizations of H. However, encouraged by the reviewer, we decided to compare the results of the various DEA-EOMCC calculations for methylene, summarized in Table 2, with their CI analogues, where we diagonalize the bare Hamiltonian in the spaces used in the DEA-EOMCC calculations. The results are shown in Table 3. In abbreviating the various CI methods, we use the same convention as that used in the DEA-EOMCC case. Thus, CI(3p-1h) stands for the CI diagonalization of the Hamiltonian in the space of 2p determinants $|\Phi^{ab}\rangle$ and 3p-1h determinants $|\Phi^{abc}_k\rangle$, whereas CI(3p-1h,4p-2h){N_u} designates the CI calculation in the space of all 2p determinants $|\Phi^{ab}\rangle$ and a subset of 3p-1h and 4p-2h determinants, $|\Phi^{\mathbf{A}bc}_k\rangle$ and $|\Phi^{\mathbf{AB}cd}_{kl}\rangle$, respectively, defined using N_u active unoccupied orbitals, etc. As mentioned in Section 2.2, the CI(3p-1h,4p-2h){N_u} diagonalization has the configurational freedom similar to that of the uncontracted multireference CI considerations in the same active space. Independent of the type of orbitals employed in this work, none of the CI calculations shown in Table 3 can compete with the analogous DEA-EOMCC approaches. The typical errors obtained in the CI diagonalizations are a few times larger than those resulting from the corresponding DEA-EOMCC computations. The DEA CI and EOMCC calculations would produce identical and exact, full CI, results in the limit of including all $R_{\mu,np\text{-}(n-2)h}$ components of $R_\mu^{(+2)}$ with n = 2, ..., N in the corresponding H and $\bar{H}$ diagonalizations, but, as with other methods based on the CC theory, the convergence toward full CI in the DEA-EOMCC case is faster than in the case of CI.

It is encouraging to observe good performance of the DEA-EOMCC(3p-1h,4p-2h){N_u} method in the methylene case, but, as already pointed out above, the lower-level DEA-EOMCC calculations truncated at 3p-1h excitations are capable of providing reasonable results too. Our next examples, described in Sections 3.2 and 3.3, demonstrate the utility of the DEA-EOMCC(3p-1h,4p-2h){N_u} approach in situations where 4p-2h contributions are considerably larger than in the case of methylene.

3.2. Adiabatic Singlet−Triplet Gap in TMM. We now turn to the TMM molecule, a non-Kekulé hydrocarbon characterized by the delocalization of four π electrons over four closely spaced π-type orbitals (see, e.g., refs 87 and 98−100 for the relevant information). The four valence MOs of TMM's π network include the nondegenerate $1a_2''$, the doubly degenerate $1e''$, and the nondegenerate $2a_2''$ orbitals, when D_{3h} symmetry of the triplet ground state is used, or the $1b_1$, $1a_2$, $2b_1$, and $3b_1$ orbitals, when C_{2v} symmetry relevant to the low-lying singlet states is adopted. Because of its fascinating and challenging electronic structure, the TMM molecule has attracted a lot of attention over the years among many

DOI: 10.1021/acs.jpca.6b11393
J. Phys. Chem. A 2017, 121, 3469−3485

theoretical and experimental groups (cf. refs 51 and 52 and refs cited therein for the historical account and further information). In particular, a lot of effort has been devoted to an accurate determination of the relatively small energy gaps between the low-lying singlet and triplet states. As implied by Hund's rule and the electron paramagnetic resonance data,[101] TMM has a D_{3h}-symmetric triplet ground state, X $^3A_2'$, dominated by the $|\{core\}(1a_2'')^2\ (1e_1'')^1\ (1e_2'')^1|$ configuration (which in a C_{2v} description becomes the X $^3B_2$ state dominated by the $|\{core\}(1b_1)^2\ (1a_2)^1\ (2b_1)^1|$ configuration). The next two states in TMM's electronic spectrum are the nearly degenerate singlets stabilized by the Jahn−Teller distortion that lifts their exact degeneracy in a D_{3h} description, which have a multireference, biradical, character. The lower of the two singlets is an open-shell singlet state characterized by a C_s minimum, which can be approximated by a twisted C_{2v} structure, so this state is usually labeled as the A $^1B_1$ state. The second singlet, which interests us in this work, studied experimentally, using photoelectron spectroscopy, in ref 88, abbreviated B $^1A_1$, is a C_{2v}-symmetric state dominated by the closed-shell $|\{core\}(1b_1)^2\ (1a_2)^2|$ and $|\{core\}(1b_1)^2\ (2b_1)^2|$ determinants (see, e.g., refs 87, 98, and 99 for more information).

The highest ab initio levels of electronic structure theory applied to TMM to date reproduce the adiabatic, purely electronic energy gap between the D_{3h}-symmetric X $^3A_2'$ ground state and the C_{2v}-symmetric B $^1A_1$ excited state, which is estimated at 18.1 kcal/mol,[87] to within 1−6 kcal/mol, that is, some high-level approaches work well, but some struggle (cf. Table 6 in ref 83 for a compilation of representative examples). Our most accurate previously published[51,52] full and active-space DIP-EOMCC calculations truncated at 4h-2p excitations and the corresponding active-space DEA-EOMCC computations truncated at 4p-2h excitations using the cc-pVDZ basis set place the adiabatic B $^1A_1$ − X $^3A_2'$ gap in TMM within 1 kcal/mol from the recommended value of 18.1 kcal/mol, independent of the type of MOs used to define the corresponding wave function expansions. The DIP-EOMCC method truncated at 3h-1p excitations and its DEA-EOMCC counterpart truncated at 3p-1h terms worsen these results, producing values that are very sensitive to the type of MOs used in the calculations, which can be as good as 18.3 kcal/mol and as bad as 23.9 kcal/mol if 3h-1p and 3p-1h components are treated fully (see refs 51 and 52 and Table 4). As shown in Table 4, the use of the larger cc-pVTZ basis does not significantly alter these conclusions; that is, the highest-level affordable DEA-EOMCC/cc-pVTZ calculations with a full treatment of 3p-1h contributions and an active-space treatment of 4p-2h terms (as already mentioned, the corresponding full DEA-EOMCC(4p-2h) calculations are prohibitively expensive for us at this time) produce the adiabatic gaps between the B $^1A_1$ and X $^3A_2'$ states in the narrow 18.4−18.7 kcal/mol range, in excellent agreement with the recommended value of 18.1 kcal/mol, whereas the DEA-EOMCC approach truncated at 3p-1h excitations treated fully gives generally less accurate values that vary from 21.1 to 23.5 kcal/mol. Our goal is to examine if we can reproduce the high-accuracy results provided by the DEA-EOMCC method with a full treatment of 3p-1h and an active-space treatment of 4p-2h terms, summarized in Table 4, with the considerably less expensive (cf. Table 1) DEA-EOMCC(3p-1h,4p-2h)$\{N_u\}$ approach. We also investigate if it is sufficient to handle 3p-1h excitations within the DEA-EOMCC schemes truncated at 3p-1h or 4p-2h components, which in refs 51 and 52 were treated fully, using a small subset of active orbitals. As in our earlier work,[51,52] in performing the DEA-EOMCC calculations with the full and active-space treatments of 3p-1h excitations and the active-space treatment of 4p-2h contributions, we adopted the geometries of the X $^3A_2'$ and B $^1A_1$ states of TMM optimized at the SF-DFT/6-31G(d) level in ref 87.

In all of the DEA-EOMCC calculations for TMM reported in this study, the $(N-2)$-electron closed-shell TMM^{2+} reference system was obtained by vacating the doubly degenerate 1e″ shell (the D_{3h}-symmetric X $^3A_2'$ state) or the nondegenerate $1a_2$ and $2b_1$ orbitals (the C_{2v}-symmetric B $^1A_1$ state) of the TMM's valence π network. To examine the dependence of the various DEA-EOMCC results on the type of MO basis that defines the corresponding wave function expansions, we used both the ground-state RHF orbitals of the TMM^{2+} reference dication and the RHF or ROHF orbitals optimized for the TMM target species. When utilizing the orbitals optimized for TMM, we followed refs 51 and 52 and adopted two different strategies. In the first strategy in this category, we relied on only one type of orbitals, namely, the high-spin ROHF MOs optimized for the triplet ground state, which we used to perform the DEA-EOMCC calculations for both electronic states of TMM that are examined here. In the second strategy, we used two different sets of MOs, namely, the ROHF orbitals optimized for the X $^3A_2'$ state in the DEA-EOMCC calculations for this D_{3h}-symmetric triplet ground state and the RHF orbitals obtained for the B $^1A_1$ state in the DEA-EOMCC calculations for the C_{2v}-symmetric B $^1A_1$ state. As already alluded to above, the third possibility of exploiting the RHF MOs optimized for the B $^1A_1$ state in the DEA-EOMCC calculations for both states of TMM that interest us here was not pursued, since such orbitals break the degeneracy of the valence 1e″ shell at the D_{3h} geometry of the triplet ground state, resulting in a symmetry-broken description of the X $^3A_2'$ state. Consistent with the structure of the valence shells of TMM, for each choice of the MO basis, the active orbitals employed in the DEA-EOMCC(3p-1h)$\{N_u\}$, DEA-EOMCC(3p-1h,4p-2h)$\{N_u\}$, and DEA-EOMCC(4p-2h)$\{N_u\}$ calculations were the doubly degenerate 1e″ and nondegenerate $2a_2''$ MOs in the case of the D_{3h}-symmetric X $^3A_2'$ state and the $1a_2$, $2b_1$, and $3b_1$ orbitals for the C_{2v}-symmetric B $^1A_1$ state, that is, N_u was set at 3, making all of these calculations affordable, even when the cc-pVTZ basis set is employed. As shown in Table 1 and as discussed in Section 2.3, this is particularly true in the case of the DEA-EOMCC(3p-1h)$\{N_u\}$ and DEA-EOMCC(3p-1h,4p-2h)$\{N_u\}$ methods, which are substantially less expensive than the corresponding DEA-EOMCC(3p-1h) and DEA-EOMCC(4p-2h)$\{N_u\}$ approaches, not to mention full DEA-EOMCC(4p-2h), which becomes prohibitively expensive for TMM.

It is apparent from Table 4 that the agreement between the adiabatic B $^1A_1$ − X $^3A_2'$ gap values obtained in the inexpensive DEA-EOMCC(3p-1h){3} calculations, which use only three active unoccupied orbitals to select the dominant 3p-1h excitations, and their counterparts obtained with the considerably more demanding DEA-EOMCC(3p-1h) approach, where 3p-1h excitations are treated fully, is generally very good. Independent of the basis set and independent of the type of MOs used to construct the corresponding wave function expansions, the differences between the active-space DEA-EOMCC(3p-1h){3} and full DEA-EOMCC(3p-1h) data do not exceed 1.2 kcal/mol, and they are, in most cases, considerably smaller, on the order of 0.2−0.6 kcal/mol. The

DOI: 10.1021/acs.jpca.6b11393
J. Phys. Chem. A 2017, 121, 3469−3485

same is observed when we compare the higher-level DEA-EOMCC(3p-1h,4p-2h){3} and DEA-EOMCC(4p-2h){3} methods, which use active orbitals to select the dominant 4p-2h contributions, but differ in the treatment of 3p-1h component of the electron attaching operator $R_{\mu}^{(+2)}$. The differences between the B $^1A_1$ − X $^3A_2'$ gap values obtained in the DEA-EOMCC(4p-2h){3} computations, where 3p-1h component is treated fully, with their counterparts obtained with the considerably less expensive DEA-EOMCC-(3p-1h,4p-2h){3} approach vary between 0.1 and 1.2 kcal/mol, with the majority of these differences falling into the 0.1−0.5 kcal/mol range. On the basis of the comparison of the full DEA-EOMCC(3p-1h), active-space DEA-EOMCC(4p-2h){3}, and experimentally derived data for the adiabatic separation between the X $^3A_2'$ and B $^1A_1$ states in TMM, 4p-2h effects are important if we are to obtain a fully quantitative description. The DEA-EOMCC(3p-1h,4p-2h){3} calculations reflect on this in a proper manner by improving the results of the DEA-EOMCC(3p-1h){3} and DEA-EOMCC(3p-1h) calculations by ∼1−5 kcal/mol, with the largest error reductions observed when the $(N-2)$-electron ionic orbitals are employed. Indeed, when one uses the RHF MOs optimized for the TMM^{2+} dication, the DEA-EOMCC(3p-1h,4p-2h){3} approach brings the results of the DEA-EOMCC(3p-1h){3} and DEA-EOMCC(3p-1h) calculations, which neglect 4p-2h correlations, closer to the recommended B $^1A_1$ − X $^3A_2'$ gap value of 18.1 kcal/mol by 4.9 and 4.6 kcal/mol, respectively, when the cc-pVDZ basis set is employed, and 5.1 and 4.6 kcal/mol, when the cc-pVTZ basis set is exploited. As a result, the adiabatic gaps between the X $^3A_2'$ and B $^1A_1$ states obtained in the DEA-EOMCC(3p-1h,4p-2h){3} calculations, which range from 18.7 and 19.4 kcal/mol, when the cc-pVDZ basis set is used, and 18.9 and 19.9 kcal/mol, when one uses the cc-pVTZ basis, are generally in very good agreement with the experimentally derived value of 18.1 kcal/mol. They are only slightly worse than the corresponding DEA-EOMCC(4p-2h){3} results, which range from 18.6 and 19.0 kcal/mol in the cc-pVDZ case and 18.4 and 18.7 kcal/mol when the cc-pVTZ basis is employed.

In analogy to the DEA-EOMCC(4p-2h){3} approach, the improvements offered by its less expensive DEA-EOMCC-(3p-1h,4p-2h){3} counterpart over the DEA-EOMCC calculations truncated at 3p-1h excitations can also be seen when we compare the sensitivity of the various DEA-EOMCC calculations to the type of orbitals used to construct the corresponding wave function expansions. Indeed, when we probe the $(N-2)$-electron MOs obtained in the RHF calculations for the TMM^{2+} reference dication and the N-electron ROHF or ROHF and RHF orbitals optimized for the TMM target system, the variation in the DEA-EOMCC(3p-1h){3} and DEA-EOMCC(3p-1h) results for the adiabatic B $^1A_1$ − X $^3A_2'$ gap in TMM is 4.6 and 4.5 kcal/mol, respectively, when the cc-pVDZ basis set is employed, and 1.7 and 2.4 kcal/mol, when one uses cc-pVTZ. DEA-EOMCC(4p-2h){3} reduces these variations to the impressively small 0.3−0.4 kcal/mol level, but it is encouraging to observe that the considerably less expensive DEA-EOMCC-(3p-1h,4p-2h){3} computations, in which the resulting gap values vary by 0.7 kcal/mol in the cc-pVDZ case and 1.0 kcal/mol in the case of cc-pVTZ, remain rather insensitive to the type of MOs used in the calculations.

3.3. Vertical Singlet−Triplet Gaps in CBD and CPC Biradicals. Continuing on the topic of biradical π systems, we also applied the DEA-EOMCC(3p-1h){N_u} and DEA-EOMCC(3p-1h,4p-2h){N_u} approaches and their more expensive full DEA-EOMCC(3p-1h) and active-space DEA-EOMCC(4p-2h){N_u} counterparts to the vertical energy gaps between the lowest singlet and triplet states in the antiaromatic CBD (C_4H_4) and CPC [$(C_5H_5)^+$] species (see Table 5). In doing so, we followed the computational strategy of ref 89. Thus, we used the cc-pVDZ basis set and adopted the D_{4h}-symmetric (CBD) and D_{5h}-symmetric (CPC) geometries of the corresponding lowest-energy triplet states optimized in ref 89. Assuming these geometries, the ground electronic states of CBD and CPC are singlet and triplet, respectively, that is, the vertical singlet−triplet gaps, $\Delta E_{S-T} = E(S) - E(T)$, which interest us in this work, should be negative for CBD and positive for CPC.

The CBD system is characterized by the delocalization of four π electrons over four π MOs, which in a D_{4h} description include the nondegenerate doubly occupied a_{2u} orbital, the doubly degenerate e_g shell, where each component orbital is singly occupied, and the unoccupied b_{2u} orbital. When the two valence e_g electrons have identical projections of the spin, one ends up with the high-spin triplet state. The corresponding singlet state is obtained when the valence e_g electrons have opposite spins recoupled to an open-shell singlet configuration. The CPC system is characterized by the delocalization of four π electrons over five π MOs, which in a D_{5h} description include the nondegenerate doubly occupied a_2'' orbital, the doubly degenerate e_1'' shell, where each component orbital is singly occupied, and the doubly degenerate unoccupied e_2'' shell. Once again, if the two valence e_1'' electrons have identical projections of the spin, one ends up with the high-spin triplet state. The singlet state is obtained when the e_1'' electrons have opposite spins recoupled to a singlet.

In analogy to TMM, the $CBD^{2+} \equiv (C_4H_4)^{2+}$ and $CPC^{2+} \equiv (C_5H_5)^{3+}$ closed-shell reference systems used in the DEA-EOMCC calculations for the CBD and CPC species reported in Table 5 were obtained by vacating the doubly degenerate valence π orbitals of each of the two target molecules. This meant vacating the highest singly occupied MOs of e_g symmetry in the case of the D_{4h}-symmetric CBD molecule and the highest singly occupied orbitals of e_1'' symmetry in the D_{5h}-symmetric CPC species. Since we already discussed the effect of using different types of MOs in the DEA-EOMCC calculations, which is relatively small when 4p-2h excitations are included, all DEA-EOMCC calculations for CBD and CPC discussed in this section were performed using only one type of orbitals, namely, the RHF MOs optimized for the CBD^{2+} and CPC^{2+} reference systems. Consistent with the structure of the valence shells of the D_{4h}-symmetric CBD species, as described above, the active orbitals employed in the DEA-EOMCC(3p-1h){N_u}, DEA-EOMCC(3p-1h,4p-2h){N_u}, and DEA-EOMCC(4p-2h){N_u} calculations for the singlet−triplet gap in CBD included the $N_u = 3$ lowest-energy unoccupied π MOs in the CBD^{2+} reference system, that is, the two orbitals of the doubly degenerate e_g shell, which was vacated when forming CBD^{2+} from CBD, and the nondegenerate b_{2u} orbital, which is empty in CBD^{2+} and CBD. Similarly, the active space used in the DEA-EOMCC(3p-1h){N_u}, DEA-EOMCC(3p-1h,4p-2h){N_u}, and DEA-EOMCC(4p-2h){N_u} calculations for the singlet−triplet gap in the D_{5h}-symmetric CPC species consisted of the $N_u = 4$ lowest-energy unoccupied π MOs in the CPC^{2+} reference system, including the doubly degenerate e_1'' shell,

DOI: 10.1021/acs.jpca.6b11393
J. Phys. Chem. A 2017, 121, 3469−3485

which was vacated when forming CPC^{2+} from CPC, and the doubly degenerate e_2'' shell, which is empty in CPC^{2+} and CPC.

The results in Table 5 clearly demonstrate that the vertical singlet−triplet gaps in the CBD and CPC systems obtained in the inexpensive active-space DEA-EOMCC(3p-1h){3} and DEA-EOMCC(3p-1h){4} calculations are in virtually perfect agreement with the corresponding full DEA-EOMCC(3p-1h) data. Indeed, the difference between the DEA-EOMCC(3p-1h){3} and DEA-EOMCC(3p-1h) ΔE_{S-T} values in CBD and the analogous difference between the results of the DEA-EOMCC(3p-1h){4} and DEA-EOMCC(3p-1h) calculations for CPC are 0.05 and 0.32 kcal/mol, respectively. The similarly small differences in the calculated ΔE_{S-T} values are observed when the results of the DEA-EOMCC(3p-1h,4p-2h){3} calculations for CBD and the results of the analogous DEA-EOMCC(3p-1h,4p-2h){4} calculations for CPC, in which 3p-1h and 4p-2h components of the electron attaching operator $R_\mu^{(+2)}$ are selected using active orbitals, are compared with the corresponding DEA-EOMCC(4p-2h){3} and DEA-EOMCC(4p-2h){4} computations, in which 3p-1h excitations are treated fully. This shows once again that the economical, active-space treatment of 3p-1h contributions advocated in this study provides us with a faithful representation of these important correlation effects.

The results in Table 5 also confirm that high-order 4p-2h effects can be quite large in biradical π systems. We saw this when examining the singlet−triplet gap in TMM, and we see it again when determining the singlet−triplet gaps in CBD and CPC. Indeed, in the case of the D_{4h}-symmetric CBD species, we observe a nearly 4 kcal/mol lowering of the calculated ΔE_{S-T} value, which stabilizes the singlet state, when 4p-2h contributions are included in the DEA-EOMCC calculations. The effect of 4p-2h correlations is smaller in the CPC case, lowering the ΔE_{S-T} value obtained in the DEA-EOMCC(3p-1h){4} and DEA-EOMCC(3p-1h) calculations by ∼2 kcal/mol, but it is still quite important. Because of prohibitive computer costs, we could not perform the corresponding full DEA-EOMCC(4p-2h) calculations, but based on the results for methylene discussed in Section 3.1, our earlier benchmark DEA-EOMCC calculations,[51,52] and experience with using the various active-space CC,[56−67] EOMCC,[68−73] and EA/IP-EOMCC[28−30,43] methods, which are known for their ability to recover relative and excitation energies of the parent CC/EOMCC calculations, often to within fractions of kilocalorie per mole (see ref 74 for a review), we may expect that the ΔE_{S-T} values for CBD obtained in the DEA-EOMCC(3p-1h,4p-2h){3} and DEA-EOMCC(4p-2h){3} calculations and the ΔE_{S-T} values for CPC resulting from the DEA-EOMCC(3p-1h,4p-2h){4} and DEA-EOMCC(4p-2h){4} computations are almost identical to the corresponding full DEA-EOMCC(4p-2h) data, which should in turn be virtually exact.

High accuracy of the DEA-EOMCC(3p-1h,4p-2h)$\{N_u\}$ and DEA-EOMCC(4p-2h)$\{N_u\}$ approaches, which include sophisticated 4p-2h terms, in addition to their lower-rank 2p and 3p-1h counterparts, on top of CCSD, implies that we should be able to treat the DEA-EOMCC(3p-1h,4p-2h){3} and DEA-EOMCC(4p-2h){3} results for CBD and the analogous DEA-EOMCC(3p-1h,4p-2h){4} and DEA-EOMCC(4p-2h){4} results for CPC, reported in Table 5, as practically converged with respect to the relevant many-electron correlation effects, allowing us to use them to judge other methods. For example, the unrestricted, symmetry-broken calculations using the single-reference CC approach with singles, doubles, and noniterative quasi-perturbative triples (CCSD(T))[102] and its Brueckner-orbital BCCD(T) analogue,[103] and the state-specific multi-reference CC calculations with singles and doubles using the MkCCSD approach of ref 104 applied to the D_{5h}-symmetric CPC species considered in this work produce ΔE_{S-T} values that are (with an exception of one, seemingly erratic, MkCCSD result) in the 13.5−14.8 kcal/mol range,[89] in excellent agreement with our DEA-EOMCC(3p-1h,4p-2h){4} and DEA-EOMCC(4p-2h){4} results in Table 5, which are 14.3 and 13.9 kcal/mol, respectively. However, when the MkCCSD method is applied to the D_{4h}-symmetric CBD system, one obtains ΔE_{S-T} values that vary from −9.0 to −8.1 kcal/mol[89] and that do not agree with our best DEA-EOMCC(3p-1h,4p-2h){3} and DEA-EOMCC(4p-2h){3} calculations, which give −5.0 kcal/mol. At the same time, as shown in ref 89, the unrestricted, symmetry-broken CCSD(T) and BCCD(T) calculations and the multireference averaged quadratic CC (MR-AQCC) approach[105,106] produce the vertical singlet−triplet gaps in the D_{4h}-symmetric CBD species that range from −5.5 to −4.8 kcal/mol, in perfect agreement with our DEA-EOMCC(3p-1h,4p-2h){3} and DEA-EOMCC(4p-2h){3} data. On the basis of our experiences with the DEA-EOMCC calculations including high-rank 4p-2h excitations, such as those described in this paper and the earlier work,[51,52] we are quite confident that the MkCCSD ΔE_{S-T} values for the D_{4h}-symmetric CBD system reported in ref 89 are in error, whereas the corresponding unrestricted CCSD(T) and BCCD(T) data and their MR-AQCC counterpart, reported in ref 89 as well, are correct. It is quite possible that the failure of the MkCCSD approach in this case is a consequence of neglecting the connected triples in the MkCCSD calculations. Indeed, as shown in ref 89, the MkCCSD values of ΔE_{S-T} for the D_{4h}-symmetric CBD system are almost identical to the results of the unrestricted, symmetry-broken, single-reference CCSD calculations. Normally, in the absence of independent information, we would be forced to speculate which of the ΔE_{S-T} values for CBD reported in ref 89 are correct. The DEA-EOMCC(3p-1h,4p-2h){3} and DEA-EOMCC(4p-2h){3} results given in Table 5, which are expected to be nearly exact, solve this problem. This is an example of the kinds of things we can do having access to the high-level DEA-EOMCC(3p-1h,4p-2h)$\{N_u\}$ and DEA-EOMCC(4p-2h)$\{N_u\}$ or at least DEA-EOMCC(3p-1h,4p-2h)$\{N_u\}$ data, which we will be able to produce in many cases because of the use of the active-space ideas to select the dominant 4p-2h or 3p-1h and 4p-2h contributions. Encouraged by the above results, especially those obtained with the high-level and yet relatively inexpensive DEA-EOMCC(3p-1h,4p-2h)$\{N_u\}$ approach, we are planning to extend the DEA-EOMCC(3p-1h)$\{N_u\}$, DEA-EOMCC(3p-1h), DEA-EOMCC(3p-1h,4p-2h)$\{N_u\}$, and DEA-EOMCC(4p-2h)$\{N_u\}$ calculations for the CBD and CPC biradicals discussed here to other antiaromatic molecules examined in ref 89.

3.4. F−F Bond Dissociation in the Fluorine Molecule.

Our final example is the potential energy curve of the challenging F_2 molecule, as described by the DZ basis set, for which the results of the exact, full CI calculations were reported in ref 91 and which was examined by us earlier, using the full DEA-EOMCC(3p-1h) and DEA-EOMCC(4p-2h) and active-space DEA-EOMCC(4p-2h)$\{N_u\}$ approaches and their DIP counterparts[51] (see Table 6). As in the other examples in this section, our discussion focuses on a comparison of the active-space DEA-EOMCC(3p-1h)$\{N_u\}$ approach with its full DEA-

DOI: 10.1021/acs.jpca.6b11393
J. Phys. Chem. A 2017, 121, 3469−3485

EOMCC(3p-1h) parent and on the ability of the DEA-EOMCC(3p-1h,4p-2h)$\{N_u\}$ method to reproduce the corresponding DEA-EOMCC(4p-2h) and DEA-EOMCC(4p-2h)$\{N_u\}$ results. Following refs 51 and 91, all of the DEA-EOMCC calculations for F_2 reported in this article use the RHF orbitals of the target species. The corresponding closed-shell reference F_2^{2+} system, needed to set up the various DEA-EOMCC calculations summarized in Table 6, was obtained by vacating the valence σ_g orbital, which is doubly occupied in the RHF determinant for F_2. The active orbitals used in the DEA-EOMCC(3p-1h)$\{N_u\}$, DEA-EOMCC(3p-1h,4p-2h)$\{N_u\}$, and DEA-EOMCC(4p-2h)$\{N_u\}$ computations consisted of the valence σ_g and σ_u MOs involved in the dissociation of the fluorine molecule, which are empty in the reference F_2^{2+} system, as defined above, that is, N_u was set at 2.

As established in our earlier study[51] and as shown in Table 6, 4p-2h excitations, treated fully or with active orbitals, play a substantial role in improving the results of the DEA-EOMCC calculations, offering a considerably more accurate description of bond breaking in F_2 than that provided by the DEA-EOMCC(3p-1h) approach. Indeed, the full DEA-EOMCC(4p-2h) and active-space DEA-EOMCC(4p-2h)$\{2\}$ approaches reduce the relatively large NPE value relative to full CI characterizing the DEA-EOMCC(3p-1h) potential energy curve of F_2, of 5.432 millihartree (mHa), to as little as 1.686 and 2.193 mHa, respectively. The considerably less expensive DEA-EOMCC(3p-1h,4p-2h)$\{2\}$ calculations are capable of maintaining these high accuracies, providing the NPE of 2.206 mHa, which is in excellent agreement with the NPEs provided by the parent DEA-EOMCC(4p-2h)$\{2\}$ and DEA-EOMCC(4p-2h) calculations. The largest errors relative to full CI, represented in Table 6 by the MUE values, do not change much when going from the DEA-EOMCC(3p-1h) to the DEA-EOMCC(3p-1h,4p-2h)$\{2\}$, DEA-EOMCC(4p-2h)$\{2\}$, and DEA-EOMCC(4p-2h) levels, but the potential energy curves obtained with the latter three approaches are much more parallel to the full CI curve than the curve obtained in the DEA-EOMCC(3p-1h) calculations. As a result, if we define the energy difference $D_e \equiv E(4R_e) - E(R_e)$ as a measure of the dissociation energy characterizing the F_2 molecule, where R_e is the equilibrium geometry, we can see an excellent agreement between the DEA-EOMCC(3p-1h,4p-2h)$\{2\}$, DEA-EOMCC(4p-2h)$\{2\}$, and DEA-EOMCC(4p-2h) D_e values, which are 13.23, 13.24, and 13.62 kcal/mol, respectively, and full CI, which gives D_e = 14.62 kcal/mol. Given its relatively low computer cost compared to the remaining two DEA-EOMCC approaches including 4p-2h excitations considered in this study, the good performance of the DEA-EOMCC(3p-1h,4p-2h)$\{2\}$ method with an active-space treatment of both 3p-1h and 4p-2h components is most encouraging.

The DEA-EOMCC(3p-1h) result for D_e, as defined above, of 17.68 kcal/mol, is substantially worse, largely because of the increase in the corresponding NPE value, from a 2 mHa level in the DEA-EOMCC(3p-1h,4p-2h)$\{2\}$, DEA-EOMCC(4p-2h)$\{2\}$, and DEA-EOMCC(4p-2h) calculations to 5.432 mHa in the DEA-EOMCC(3p-1h) case, but the good news is that the active-space DEA-EOMCC(3p-1h)$\{2\}$ approach provides the energetics of full DEA-EOMCC(3p-1h) at the small fraction of the computer cost. Indeed, the DEA-EOMCC(3p-1h)$\{2\}$ values of NPE and D_e, which are 5.398 mHa and 17.64 kcal/mol, respectively, are in perfect agreement with their full DEA-EOMCC(3p-1h) counterparts. The inexpensive active-space treatment of 3p-1h excitations, which we advocate in this study, is clearly sufficient to capture the relevant 3p-1h correlation effects.

4. SUMMARY AND CONCLUDING REMARKS

We have demonstrated that the previously developed DEA-EOMCC approaches with full and active-space treatments of 4p-2h excitations, abbreviated as DEA-EOMCC(4p-2h) and DEA-EOMCC(4p-2h)$\{N_u\}$, respectively,[51,52] which represent state-of-the-art methodologies within the DEA-EOMCC framework and which are particularly well-suited to describe electronic structure and spectra of biradical systems and single bond breaking in closed-shell molecules leading to doublet radical fragments, can be made considerably more economical if the corresponding 3p-1h contributions are treated using active orbitals. The resulting DEA-EOMCC(3p-1h,4p-2h)$\{N_u\}$ approach, developed and implemented in this work, replaces the expensive $\mathcal{N}^6$-like $n_o n_u^5$ steps associated with 3p-1h excitations by the much less time-consuming $\mathcal{N}^5$-like $N_u n_o n_u^4$ operations, where N_u is the number of active unoccupied orbitals in the underlying $(N-2)$-electron closed-shell core, in addition to downscaling the prohibitively expensive $\mathcal{N}^8$-like $n_o^2 n_u^6$ steps associated with 4p-2h contributions to a manageable $\mathcal{N}^6$-like $N_u^2 n_o^2 n_u^4$ level. By examining the low-lying singlet and triplet states of methylene, trimethylenemethane, cyclobutadiene, and cyclopentadienyl cation and bond breaking in F_2, we have demonstrated that the DEA-EOMCC(3p-1h,4p-2h)$\{N_u\}$ method is practically as accurate as its parent DEA-EOMCC(4p-2h)$\{N_u\}$ and DEA-EOMCC(4p-2h) models at the fraction of the computational cost involved in the DEA-EOMCC(4p-2h)$\{N_u\}$ and DEA-EOMCC(4p-2h) calculations, while preserving all other features of the DEA-EOMCC methodology, such as rigorous spin and symmetry adaptation, which are difficult to achieve within the standard particle-conserving CC/EOMCC framework. We have also demonstrated that the DEA-EOMCC(3p-1h,4p-2h)$\{N_u\}$ scheme is almost as insensitive to the choice of the underlying MO basis used in the calculations as the considerably more expensive DEA-EOMCC(4p-2h)$\{N_u\}$ and DEA-EOMCC(4p-2h) approaches.

The methodological advances reported in this article have also benefited the lower-level DEA-EOMCC approach truncated at 3p-1h excitations, which can be useful in applications involving biradicals too, by replacing the $n_o n_u^5$ steps associated with a full treatment of 3p-1h contributions by the much less demanding $N_u n_o n_u^4$ steps of the active-space DEA-EOMCC(3p-1h)$\{N_u\}$ approach, implemented in this work as well. Just like its DEA-EOMCC(3p-1h) parent, the DEA-EOMCC(3p-1h)$\{N_u\}$ model with an active-space treatment of 3p-1h excitations, which ignores 4p-2h correlation effects, is less accurate than the DEA-EOMCC(3p-1h,4p-2h)$\{N_u\}$, DEA-EOMCC(4p-2h)$\{N_u\}$, and DEA-EOMCC(4p-2h) methods, but it faithfully reproduces the results of DEA-EOMCC(3p-1h) calculations at the small fraction of the computer cost, offering a useful alternative to the DEA-EOMCC(3p-1h) approximation, where 3p-1h terms are treated fully.

AUTHOR INFORMATION

Corresponding Author

*E-mail: piecuch@chemistry.msu.edu.

ORCID

Piotr Piecuch: 0000-0002-7207-1815

DOI: 10.1021/acs.jpca.6b11393
J. Phys. Chem. A 2017, 121, 3469−3485

Notes

The authors declare no competing financial interest.

■ ACKNOWLEDGMENTS

This work has been supported by the Chemical Sciences, Geosciences and Biosciences Division, Office of Basic Energy Sciences, Office of Science, U.S. Department of Energy (Grant No. DE-FG02-01ER15228). We thank Profs. L. Gagliardi and D. G. Truhlar and Mr. S. J. Stoneburner for useful discussions.

■ REFERENCES

(1) Hubbard, J. The Description of Collective Motions in Terms of Many-Body Perturbation Theory. *Proc. R. Soc. London, Ser. A* **1957**, *240*, 539−560.
(2) Hugenholtz, N. M. Perturbation Theory of Large Quantum Systems. *Physica* **1957**, *23*, 481−532.
(3) Coester, F. Bound States of a Many-Particle System. *Nucl. Phys.* **1958**, *7*, 421−424.
(4) Coester, F.; Kümmel, H. Short-Range Correlations in Nuclear Wave Functions. *Nucl. Phys.* **1960**, *17*, 477−485.
(5) Čížek, J. On the Correlation Problem in Atomic and Molecular Systems. Calculation of Wavefunction Components in Ursell-Type Expansion using Quantum-Field Theoretical Methods. *J. Chem. Phys.* **1966**, *45*, 4256−4266.
(6) Čížek, J. On the use of the Cluster Expansion and the Technique of Diagrams in Calculations of Correlation Effects in Atoms and Molecules. *Adv. Chem. Phys.* **1969**, *14*, 35−89.
(7) Čížek, J.; Paldus, J. Correlation Problems in Atomic and Molecular Systems. III. Rederivation of the Coupled-Pair Many-Electron Theory using the Traditional Quantum Chemical Methods. *Int. J. Quantum Chem.* **1971**, *5*, 359−379.
(8) Paldus, J.; Čížek, J.; Shavitt, I. Correlation Problems in Atomic and Molecular Systems. IV. Extended Coupled-Pair Many-Electron Theory and its Application to the BH_3 Molecule. *Phys. Rev. A: At., Mol., Opt. Phys.* **1972**, *5*, 50−67.
(9) Emrich, K. An Extension of the Coupled Cluster Formalism to Excited States (I). *Nucl. Phys. A* **1981**, *351*, 379−396.
(10) Geertsen, J.; Rittby, M.; Bartlett, R. J. The Equation-of-Motion Coupled-Cluster Method: Excitation Energies of Be and CO. *Chem. Phys. Lett.* **1989**, *164*, 57−62.
(11) Comeau, D. C.; Bartlett, R. J. The Equation-of-Motion Coupled-Cluster Method. Applications to Open- and Closed-Shell Reference States. *Chem. Phys. Lett.* **1993**, *207*, 414−423.
(12) Stanton, J. F.; Bartlett, R. J. The Equation of Motion Coupled-Cluster Method. A Systematic Biorthogonal Approach to Molecular Excitation Energies, Transition Probabilities, and Excited State Properties. *J. Chem. Phys.* **1993**, *98*, 7029−7039.
(13) Piecuch, P.; Bartlett, R. J. EOMXCC: A New Coupled-Cluster Method for Electronic Excited States. *Adv. Quantum Chem.* **1999**, *34*, 295−380.
(14) Monkhorst, H. J. Calculation of Properties with the Coupled-Cluster Method. *Int. J. Quantum Chem. Symp.* **1977**, *11*, 421−432.
(15) Dalgaard, E.; Monkhorst, H. J. Some Aspects of the Time-Dependent Coupled-Cluster Approach to Dynamic Response Functions. *Phys. Rev. A: At., Mol., Opt. Phys.* **1983**, *28*, 1217−1222.
(16) Mukherjee, D.; Mukherjee, P. K. A Response-Function Approach to the Direct Calculation of the Transition-Energy in a Multiple-Cluster Expansion Formalism. *Chem. Phys.* **1979**, *39*, 325−335.
(17) Takahashi, M.; Paldus, J. Time-Dependent Coupled Cluster Approach: Excitation Energy Calculation Using an Orthogonally Spin-Adapted Formalism. *J. Chem. Phys.* **1986**, *85*, 1486−1501.
(18) Koch, H.; Jørgensen, P. Coupled Cluster Response Functions. *J. Chem. Phys.* **1990**, *93*, 3333−3344.
(19) Koch, H.; Jensen, H. J. A.; Jørgensen, P.; Helgaker, T. Excitation Energies from the Coupled Cluster Singles and Doubles Linear Response Function (CCSDLR). Applications to Be, CH^+, CO, and H_2O. *J. Chem. Phys.* **1990**, *93*, 3345−3350.
(20) Kondo, A. E.; Piecuch, P.; Paldus, J. Orthogonally Spin-Adapted Single-Reference Coupled-Cluster Formalism: Linear Response Calculation of Static Properties. *J. Chem. Phys.* **1995**, *102*, 6511−6524.
(21) Kondo, A. E.; Piecuch, P.; Paldus, J. Orthogonally Spin-Adapted Single-Reference Coupled-Cluster Formalism: Linear Response Calculation of Higher-Order Static Properties. *J. Chem. Phys.* **1996**, *104*, 8566−8585.
(22) Paldus, J.; Li, X. A Critical Assessment of Coupled Cluster Method in Quantum Chemistry. *Adv. Chem. Phys.* **1999**, *110*, 1−175.
(23) Bartlett, R. J.; Musiał, M. Coupled-cluster Theory in Quantum Chemistry. *Rev. Mod. Phys.* **2007**, *79*, 291−352.
(24) Nooijen, M.; Bartlett, R. J. Equation of Motion Coupled Cluster Method for Electron Attachment. *J. Chem. Phys.* **1995**, *102*, 3629−3647.
(25) Nooijen, M.; Bartlett, R. J. Description of Core-Excitation Spectra by the Open-Shell Electron-Attachment Equation-of-Motion Coupled Cluster Method. *J. Chem. Phys.* **1995**, *102*, 6735−6756.
(26) Hirata, S.; Nooijen, M.; Bartlett, R. J. High-Order Determinantal Equation-of-Motion Coupled-Cluster Calculations for Ionized and Electron-Attached States. *Chem. Phys. Lett.* **2000**, *328*, 459−468.
(27) Musiał, M.; Bartlett, R. J. Equation-of-Motion Coupled Cluster Method with Full Inclusion of Connected Triple Excitations for Electron-Attached States: EA-EOM-CCSDT. *J. Chem. Phys.* **2003**, *119*, 1901−1908.
(28) Gour, J. R.; Piecuch, P.; Włoch, M. Active-Space Equation-of-Motion Coupled-Cluster Methods for Excited States of Radicals and other Open-Shell Systems: EA-EOMCCSDt and IP-EOMCCSDt. *J. Chem. Phys.* **2005**, *123*, 134113.
(29) Gour, J. R.; Piecuch, P.; Włoch, M. Extension of the Active-Space Equation-of-Motion Coupled-Cluster Methods to Radical Systems: The EA-EOMCCSDt and IP-EOMCCSDt Approaches. *Int. J. Quantum Chem.* **2006**, *106*, 2854−2874.
(30) Gour, J. R.; Piecuch, P. Efficient Formulation and Computer Implementation of the Active-Space Electron-Attached and Ionized Equation-of-Motion Coupled-Cluster Methods. *J. Chem. Phys.* **2006**, *125*, 234107.
(31) Nooijen, M.; Snijders, J. G. Coupled Cluster Approach to the Single Particle Green's Function. *Int. J. Quantum Chem. Symp.* **1992**, *26*, 55−83.
(32) Nooijen, M.; Snijders, J. G. Coupled Cluster Green's Function Method: Working Equations and Applications. *Int. J. Quantum Chem.* **1993**, *48*, 15−48.
(33) Stanton, J. F.; Gauss, J. Analytic Energy Derivatives for Ionized States Described by the Equation-of-Motion Coupled-Cluster Method. *J. Chem. Phys.* **1994**, *101*, 8938−8944.
(34) Bartlett, R. J.; Stanton, J. F. In *Reviews in Computational Chemistry*; Lipkowitz, K. B., Boyd, D. B., Eds.; VCH Publishers: New York, 1994; Vol. *5*; pp 65−169.
(35) Musiał, M.; Kucharski, S. A.; Bartlett, R. J. Equation-of-Motion Coupled Cluster Method with Full Inclusion of the Connected Triple Excitations for Ionized States: IP-EOM-CCSDT. *J. Chem. Phys.* **2003**, *118*, 1128−1136.
(36) Musiał, M.; Bartlett, R. J. EOM-CCSDT Study of the Low-Lying Ionization Potentials of Ethylene, Acetylene and Formaldehyde. *Chem. Phys. Lett.* **2004**, *384*, 210−214.
(37) Bomble, Y. J.; Saeh, J. C.; Stanton, J. F.; Szalay, P. G.; Kállay, M.; Gauss, J. Equation-of-Motion Coupled-Cluster Methods for Ionized States with an Approximate Treatment of Triple Excitations. *J. Chem. Phys.* **2005**, *122*, 154107.
(38) Kamiya, M.; Hirata, S. Higher-Order Equation-of-Motion Coupled-Cluster Methods for Ionization Processes. *J. Chem. Phys.* **2006**, *125*, 074111.
(39) Ghosh, S.; Mukherjee, D.; Bhattacharyya, S. Application of Linear Response Theory in a Coupled Cluster Framework for the Calculation of Ionization Potentials. *Mol. Phys.* **1981**, *43*, 173−179.
(40) Nakatsuji, H.; Hirao, K. Cluster Expansion of the Wave Function. Electron Correlations in Singlet and Triplet Excited States, Ionized States, and Electron Attached States by SAC and SAC-CI Theories. *Int. J. Quantum Chem.* **1981**, *20*, 1301−1313.

DOI: 10.1021/acs.jpca.6b11393
J. Phys. Chem. A 2017, 121, 3469−3485

(41) Nakatsuji, H.; Ohta, K.; Yonezawa, T. Cluster Expansion of the Wave Function. Spin and Electron Correlations in Doublet Radicals Studied by the Symmetry Adapted Cluster and Symmetry Adapted Cluster-Configuration Interaction Theories. *J. Phys. Chem.* **1983**, *87*, 3068−3074.
(42) Nakatsuji, H. Description of Two- and Many-Electron Processes by the SAC-CI Method. *Chem. Phys. Lett.* **1991**, *177*, 331−337.
(43) Ohtsuka, Y.; Piecuch, P.; Gour, J. R.; Ehara, M.; Nakatsuji, H. Active-Space Symmetry-Adapted-Cluster Configuration-Interaction and Equation-of-Motion Coupled-Cluster Methods for High Accuracy Calculations of Potential Energy Surfaces of Radicals. *J. Chem. Phys.* **2007**, *126*, 164111.
(44) Nooijen, M.; Bartlett, R. J. A New Method for Excited States: Similarity Transformed Equation-of-Motion Coupled-Cluster Theory. *J. Chem. Phys.* **1997**, *106*, 6441−6448.
(45) Nooijen, M. State Selective Equation of Motion Coupled Cluster Theory: Some Preliminary Results. *Int. J. Mol. Sci.* **2002**, *3*, 656−675.
(46) Sattelmeyer, K. W.; Schaefer, H. F., III; Stanton, J. F. Use of 2h and 3h-1p-like Coupled-Cluster Tamm-Dancoff Approaches for the Equilibrium Properties of Ozone. *Chem. Phys. Lett.* **2003**, *378*, 42−46.
(47) Musiał, M.; Perera, A.; Bartlett, R. J. Multireference Coupled-Cluster Theory: The Easy Way. *J. Chem. Phys.* **2011**, *134*, 114108.
(48) Musiał, M.; Kucharski, S. A.; Bartlett, R. J. Multireference Double Electron Attached Coupled Cluster Method with Full Inclusion of the Connected Triple Excitations: MR-DA-CCSDT. *J. Chem. Theory Comput.* **2011**, *7*, 3088−3096.
(49) Kuś, T.; Krylov, A. I. Using the Charge-Stabilization Technique in the Double Ionization Potential Equation-of-Motion Calculations with Dianion References. *J. Chem. Phys.* **2011**, *135*, 084109.
(50) Kuś, T.; Krylov, A. I. De-perturbative Corrections for Charge-Stabilized Double Ionization Potential Equation-of-Motion Coupled-Cluster Method. *J. Chem. Phys.* **2012**, *136*, 244109.
(51) Shen, J.; Piecuch, P. Doubly Electron-Attached and Doubly Ionized Equation-of-Motion Coupled-Cluster Methods with 4-particle−2-hole and 4-hole−2-particle Excitations and their Active-Space Extensions. *J. Chem. Phys.* **2013**, *138*, 194102.
(52) Shen, J.; Piecuch, P. Doubly Electron-Attached and Doubly Ionised Equation-of-Motion Coupled-Cluster Methods with Full and Active-Space Treatments of 4-particle−2-hole and 4-hole−2-particle Excitations: The Role of Orbital Choices. *Mol. Phys.* **2014**, *112*, 868−885.
(53) Musiał, M.; Olszówka, M.; Lyakh, D. I.; Bartlett, R. J. The Equation-of-Motion Coupled Cluster Method for Triple Electron Attached States. *J. Chem. Phys.* **2012**, *137*, 174102.
(54) Purvis, G. D., III; Bartlett, R. J. A Full Coupled-Cluster Singles and Doubles Model: The Inclusion of Disconnected Triples. *J. Chem. Phys.* **1982**, *76*, 1910−1918.
(55) Cullen, J. M.; Zerner, M. C. The Linked Singles and Doubles Model: An Approximate Theory of Electron Correlation Based on the Coupled-Cluster Ansatz. *J. Chem. Phys.* **1982**, *77*, 4088−4109.
(56) Oliphant, N.; Adamowicz, L. Multireference Coupled-Cluster Method using a Single-Reference Formalism. *J. Chem. Phys.* **1991**, *94*, 1229−1235.
(57) Oliphant, N.; Adamowicz, L. The Implementation of the Multireference Coupled-Cluster Method Based on the Single-Reference Formalism. *J. Chem. Phys.* **1992**, *96*, 3739−3744.
(58) Piecuch, P.; Oliphant, N.; Adamowicz, L. A State-Selective Multireference Coupled-Cluster Theory Employing the Single-Reference Formalism. *J. Chem. Phys.* **1993**, *99*, 1875−1900.
(59) Piecuch, P.; Adamowicz, L. State-Selective Multi-reference Coupled-Cluster Theory using Multi-Configuration Self-Consistent-Field Orbitals. A Model Study on H_8. *Chem. Phys. Lett.* **1994**, *221*, 121−128.
(60) Piecuch, P.; Adamowicz, L. State-Selective Multireference Coupled-Cluster Theory Employing the Single-Reference Formalism: Implementation and Application to the H_8 Model System. *J. Chem. Phys.* **1994**, *100*, 5792−5809.
(61) Piecuch, P.; Adamowicz, L. Breaking Bonds with the State-Selective Multireference Coupled-Cluster Method Employing the Single-Reference Formalism. *J. Chem. Phys.* **1995**, *102*, 898−904.
(62) Ghose, K. B.; Piecuch, P.; Adamowicz, L. Improved Computational Strategy for the State-Selective Coupled-Cluster Theory with Semi-Internal Triexcited Clusters: Potential-Energy Surface of the HF Molecule. *J. Chem. Phys.* **1995**, *103*, 9331−9346.
(63) Ghose, K. B.; Adamowicz, L. Use of Recursively Generated Intermediates in State Selective Multireference Coupled-Cluster Method: A Numerical Example. *J. Chem. Phys.* **1995**, *103*, 9324−9330.
(64) Ghose, K. B.; Piecuch, P.; Pal, S.; Adamowicz, L. State-Selective Multireference Coupled-Cluster Theory: In Pursuit of Property Calculation. *J. Chem. Phys.* **1996**, *104*, 6582−6589.
(65) Adamowicz, L.; Piecuch, P.; Ghose, K. B. The State-Selective Coupled Cluster Method for Quasi-Degenerate Electronic States. *Mol. Phys.* **1998**, *94*, 225−234.
(66) Piecuch, P.; Kucharski, S. A.; Bartlett, R. J. Coupled-Cluster Methods with Internal and Semi-Internal Triply and Quadruply Excited Clusters: CCSDt and CCSDtq Approaches. *J. Chem. Phys.* **1999**, *110*, 6103−6122.
(67) Piecuch, P.; Kucharski, S. A.; Špirko, V. Coupled-Cluster Methods with Internal and Semi-Internal Triply Excited Clusters: Vibrational Spectrum of the HF Molecule. *J. Chem. Phys.* **1999**, *111*, 6679−6692.
(68) Kowalski, K.; Piecuch, P. The Active-Space Equation-of-Motion Coupled-Cluster Methods for Excited Electronic States: The EOMCCSDt Approach. *J. Chem. Phys.* **2000**, *113*, 8490−8502.
(69) Kowalski, K.; Piecuch, P. The Active-Space Equation-of-Motion Coupled-Cluster Methods for Excited Electronic States: Full EOMCCSDt. *J. Chem. Phys.* **2001**, *115*, 643−651.
(70) Kowalski, K.; Piecuch, P. Excited-State Potential Energy Curves of CH^+: A Comparison of the EOMCCSDt and Full EOMCCSDT Results. *Chem. Phys. Lett.* **2001**, *347*, 237−246.
(71) Kowalski, K.; Hirata, S.; Włoch, M.; Piecuch, P.; Windus, T. L. Active-Space Coupled-Cluster Study of Electronic States of Be_3. *J. Chem. Phys.* **2005**, *123*, 074319.
(72) Piecuch, P.; Hirata, S.; Kowalski, K.; Fan, P.-D.; Windus, T. L. Automated Derivation and Parallel Computer Implementation of Renormalized and Active-Space Coupled-Cluster Methods. *Int. J. Quantum Chem.* **2006**, *106*, 79−97.
(73) Fan, P.-D.; Hirata, S. Active-Space Coupled-Cluster Methods through Connected Quadruple Excitations. *J. Chem. Phys.* **2006**, *124*, 104108.
(74) Piecuch, P. Active-Space Coupled-Cluster Methods. *Mol. Phys.* **2010**, *108*, 2987−3015.
(75) Schmidt, M. W.; Baldridge, K. K.; Boatz, J. A.; Elbert, S. T.; Gordon, M. S.; Jensen, J. H.; Koseki, S.; Matsunaga, N.; Nguyen, K. A.; Su, S. J.; et al. General Atomic and Molecular Electronic Structure System. *J. Comput. Chem.* **1993**, *14*, 1347−1363.
(76) Gordon, M. S.; Schmidt, M. W. In *Theory and Applications of Computational Chemistry: The First Forty Years;* Dykstra, C. E., Frenking, G., Kim, K. S., Scuseria, G. E., Eds.; Elsevier: Amsterdam, 2005; pp 1167−1189.
(77) Piecuch, P.; Kucharski, S. A.; Kowalski, K.; Musiał, M. Efficient Computer Implementation of the Renormalized Coupled-Cluster Methods: The R-CCSD[T], R-CCSD(T), CR-CCSD[T], and CR-CCSD(T) Approaches. *Comput. Phys. Commun.* **2002**, *149*, 71−96.
(78) Kowalski, K.; Piecuch, P. New Coupled-Cluster Methods with Singles, Doubles, and Noniterative Triples for High Accuracy Calculations of Excited Electronic States. *J. Chem. Phys.* **2004**, *120*, 1715−1738.
(79) Włoch, M.; Gour, J. R.; Kowalski, K.; Piecuch, P. Extension of Renormalized Coupled-Cluster Methods Including Triple Excitations to Excited Electronic States of Open-Shell Molecules. *J. Chem. Phys.* **2005**, *122*, 214107.
(80) Piecuch, P.; Gour, J. R.; Włoch, M. Left-Eigenstate Completely Renormalized Equation-of-Motion Coupled-Cluster Methods: Review of Key Concepts, Extension to Excited States of Open-Shell Systems,

DOI: 10.1021/acs.jpca.6b11393
J. Phys. Chem. A 2017, 121, 3469−3485

and Comparison with Electron-Attached and Ionized Approaches. *Int. J. Quantum Chem.* **2009**, *109*, 3268−3304.
(81) Shen, J.; Piecuch, P. Biorthogonal Moment Expansions in Coupled-Cluster Theory: Review of Key Concepts and Merging the Renormalized and Active-Space Coupled-Cluster Methods. *Chem. Phys.* **2012**, *401*, 180−202.
(82) Shen, J.; Piecuch, P. Combining Active-Space Coupled-Cluster Methods with Moment Energy Corrections via the CC(*P*;*Q*) Methodology, with Benchmark Calculations for Biradical Transition States. *J. Chem. Phys.* **2012**, *136*, 144104.
(83) Shen, J.; Piecuch, P. Merging Active-Space and Renormalized Coupled-Cluster Methods via the CC(*P*;*Q*) Formalism, with Benchmark Calculations for Singlet-Triplet Gaps in Biradical Systems. *J. Chem. Theory Comput.* **2012**, *8*, 4968−4988.
(84) Dunning, T. H., Jr. Gaussian Basis Sets for Use in Correlated Molecular Calculations. I. The Atoms Boron through Neon and Hydrogen. *J. Chem. Phys.* **1989**, *90*, 1007−1023.
(85) Dunning, T. H., Jr. Gaussian Basis Functions for Use in Molecular Calculations. III. Contraction of (10s6p) Atomic Basis Sets for First-Row Atoms. *J. Chem. Phys.* **1971**, *55*, 716−723.
(86) Sherrill, C. D.; Leininger, M. L.; van Huis, T. J.; Schaefer, H. F., III Structures and Vibrational Frequencies in the Full Configuration Interaction Limit: Predictions for Four Electronic States of Methylene using a Triple-Zeta Plus Double Polarization (TZ2P) Basis. *J. Chem. Phys.* **1998**, *108*, 1040−1049.
(87) Slipchenko, L. V.; Krylov, A. I. Singlet-Triplet Gaps in Diradicals by the Spin-Flip Approach: A Benchmark Study. *J. Chem. Phys.* **2002**, *117*, 4694−4708.
(88) Wenthold, P. G.; Hu, J.; Squires, R. R.; Lineberger, W. C. Photoelectron Spectroscopy of the Trimethylenemethane Negative Ion. The Singlet-Triplet Splitting of Trimethylenemethane. *J. Am. Chem. Soc.* **1996**, *118*, 475−476.
(89) Saito, T.; Nishihara, S.; Yamanaka, S.; Kitagawa, Y.; Kawakami, T.; Yamada, S.; Isobe, H.; Okumura, M.; Yamaguchi, K. Symmetry and Broken Symmetry in Molecular Orbital Description of Unstable Molecules IV: Comparison between Single- and Multi-Reference Computational Results for Antiaromatic Molecules. *Theor. Chem. Acc.* **2011**, *130*, 749−763.
(90) Dunning, T. H., Jr. Gaussian Basis Functions for Use in Molecular Calculations. I. Contraction of (9s5p) Atomic Basis Sets for First-Row Atoms. *J. Chem. Phys.* **1970**, *53*, 2823−2833.
(91) Li, X.; Paldus, J. A Truncated Version of Reduced Multi-reference Coupled-Cluster Method with Singles and Doubles and Noniterative Triples: Application to F_2 and $Ni(CO)_n$ (n = 1, 2, and 4). *J. Chem. Phys.* **2006**, *125*, 164107.
(92) Harrison, J. F. Structure of Methylene. *Acc. Chem. Res.* **1974**, *7*, 378−384.
(93) Shavitt, I. Geometry and Singlet-Triplet Energy Gap in Methylene: A Critical Review of Experimental and Theoretical Determinations. *Tetrahedron* **1985**, *41*, 1531−1542.
(94) Goddard, W. A., III Theoretical Chemistry Comes Alive: Full Partner with Experiment. *Science* **1985**, *227*, 917−923.
(95) Schaefer, H. F., III Methylene: A Paradigm for Computational Quantum Chemistry. *Science* **1986**, *231*, 1100−1107.
(96) Bunker, P. R. In *Comparison of Ab Initio Quantum Chemistry with Experiment for Small Molecules;* Bartlett, R. J., Ed.; Reidel: Dordrecht, The Netherlands, 1985; pp 141−170.
(97) Harrison, J. F. In *Advances in the Theory of Atomic and Molecular Systems: Conceptual and Computational Advances in Quantum Chemistry;* Piecuch, P., Maruani, J., Delgado-Barrio, G., Wilson, S., Eds.; Progress in Theoretical Chemistry and Physics; Springer: Dordrecht, The Netherlands, 2009; Vol. *19*; pp 33−43.
(98) Cramer, C. J.; Smith, B. A. Trimethylenemethane. Comparison of Multiconfigurational Self-Consistent Field and Density Functional Methods for a Non-Kekulé Hydrocarbon. *J. Phys. Chem.* **1996**, *100*, 9664−9670.
(99) Slipchenko, L. V.; Krylov, A. I. Electronic Structure of the Trimethylenemethane Diradical in its Ground and Electronically Excited States: Bonding, Equilibrium Geometries, and Vibrational Frequencies. *J. Chem. Phys.* **2003**, *118*, 6874−6883.
(100) Slipchenko, L. V.; Krylov, A. I. Spin-Conserving and Spin-Flipping Equation-of-Motion Coupled-Cluster Method with Triple Excitations. *J. Chem. Phys.* **2005**, *123*, 084107.
(101) Baseman, R. J.; Pratt, D. W.; Chow, M.; Dowd, P. Trimethylenemethane. Experimental Demonstration that the Triplet State is the Ground State. *J. Am. Chem. Soc.* **1976**, *98*, 5726−5727.
(102) Raghavachari, K.; Trucks, G. W.; Pople, J. A.; Head-Gordon, M. A Fifth-Order Perturbation Comparison of Electron Correlation Theories. *Chem. Phys. Lett.* **1989**, *157*, 479−483.
(103) Raghavachari, K.; Pople, J. A.; Replogle, E. S.; Head-Gordon, M.; Handy, N. C. Size-Consistent Brueckner Theory Limited to Double and Triple Substitutions. *Chem. Phys. Lett.* **1990**, *167*, 115−121.
(104) Mahapatra, U. S.; Datta, B.; Mukherjee, D. A Size-Consistent State-Specific Multireference Coupled Cluster Theory: Formal Developments and Molecular Applications. *J. Chem. Phys.* **1999**, *110*, 6171−6188.
(105) Szalay, P. G.; Bartlett, R. J. Multi-reference Averaged Quadratic Coupled-Cluster Method: A Size-Extensive Modification of Multi-reference CI. *Chem. Phys. Lett.* **1993**, *214*, 481−488.
(106) Szalay, P. G.; Bartlett, R. J. Approximately Extensive Modifications of the Multireference Configuration Interaction Method: A Theoretical and Practical Analysis. *J. Chem. Phys.* **1995**, *103*, 3600−3612.

DOI: 10.1021/acs.jpca.6b11393
J. Phys. Chem. A 2017, 121, 3469−3485